

TOPICAL REVIEW

Neutron Reactions in Astrophysics

R. Reifarth¹, C. Lederer^{1,a}, F. Käppeler²

¹ Goethe University Frankfurt, Frankfurt, Germany

² Karlsruhe Institute of Technology, Karlsruhe, Germany

^a Present Affiliation: University of Edinburgh, Edinburgh, UK

E-mail: reifarth@physik.uni-frankfurt.de

Abstract. The quest for the origin of matter in the Universe had been the subject of philosophical and theological debates over the history of mankind, but quantitative answers could be found only by the scientific achievements of the last century. A first important step on this way was the development of spectral analysis by Kirchhoff and Bunsen in the middle of the 19th century, which provided first insight in the chemical composition of the sun and the stars. The energy source of the stars and the related processes of nucleosynthesis, however, could be revealed only with the discoveries of nuclear physics. A final breakthrough came eventually with the compilation of elemental and isotopic abundances in the solar system, which are reflecting the various nucleosynthetic processes in detail.

This review is focusing on the mass region above iron, where the formation of the elements is dominated by neutron capture, mainly in the slow (*s*) and rapid (*r*) processes. Following a brief historic account and a sketch of the relevant astrophysical models, emphasis is put on the nuclear physics input, where status and perspectives of experimental approaches are presented in some detail, complemented by the indispensable role of theory.

Contents

1	Neutron capture nucleosynthesis	2
1.1	Milestones and basic concepts	2
1.2	Solar abundances	6
2	Astrophysical models	7
2.1	The <i>s</i> process in asymptotic giant branch stars	7
2.2	The <i>s</i> process in massive stars	10
2.3	Explosive scenarios: <i>r</i> and <i>p</i> process	11
2.4	Galactic Chemical Evolution	15
3	Neutron reactions	16
3.1	Definitions and current database	16
3.2	Time-of-flight experiments	17
3.3	The activation method	22
3.4	Indirect measurements	24
4	Facilities and achievements	24
4.1	White neutron sources	24
4.2	Low-energy accelerators	26
4.3	Role of Theory	28
4.4	Stellar decay rates	30
5	Current developments and new opportunities	31
5.1	New facilities	31
5.2	Detectors	34
5.3	Advanced concepts	38
6	Status and requests	39
6.1	Compilations of stellar (<i>n, γ</i>) cross sections	39
6.2	Further requirements	40
7	Summary	42

1. Neutron capture nucleosynthesis

1.1. Milestones and basic concepts

In 1938, the quest for the energy production in stars had been solved by the work of Bethe and Critchfield [1], von Weizsäcker [2], and Bethe [3], but the origin of the heavy elements remained a puzzle for almost two more decades. It was finally the discovery of the unstable element technetium in the atmosphere of red giant stars by Merrill in 1952 [4], which settled this issue in favor of stellar nucleosynthesis, thus questioning

a primordial production in the Big Bang. A stellar origin of the heavy elements was strongly supported by the increasingly reliable compilations of the abundances in the solar system by Suess and Urey [5] and Cameron [6], because the pronounced features in the abundance distribution could be interpreted in terms of a series of nucleosynthesis scenarios associated with stellar evolution models. This key achievement is summarized in the famous fundamental papers published in 1957 by Burbidge, Burbidge, Fowler and Hoyle (B²FH) [7] and by Cameron [8, 9].

While the elements from carbon to iron were found to be produced by charged particle reactions during the evolutionary phases from stellar He to Si burning, all elements heavier than iron are essentially built up by neutron reactions in the slow (*s*) and rapid (*r*) neutron capture processes as they were termed by B²FH.

The *s* process, which takes place during He and C burning, is characterized by comparably low neutron densities, typically a few times 10^8 cm^{-3} , so that neutron capture times are much slower than most β decay times. This implies that the reaction path of the *s* process follows the stability valley as sketched in Figure 1 with the important consequence that the neutron capture cross sections averaged over the stellar spectrum are of pivotal importance for the resulting *s* abundances. Although the available cross sections under stellar conditions were very scarce and rather uncertain, already B²FH could infer that the product of cross section times the resulting *s* abundance represents a smooth function of mass number *A*. In the following decade, the information on cross section data was significantly improved by dedicated measurements [10], leading to a first compilation of stellar (*n*, γ) cross sections by Allen, Gibbons and Macklin in 1971 [11]. Meanwhile, Clayton et al. [12] had worked out a phenomenological model of the *s* process, assuming a seed abundance of ⁵⁶Fe exposed to an exponential distribution of neutron exposures with the cross section values of the involved isotopes in the reaction path as the essential input.

As the cross section database was improved, this classical model turned out to be extremely useful for describing the *s*-process component in the solar abundance distribution. In fact, it turned out that the *s* process itself was composed of different parts, i.e. the weak, main, and strong components as shown by Seeger et al. [13]. This *s*-process picture was eventually completed by the effect of important branchings in the reaction path due to the competition between neutron capture and β^- -decay of sufficiently long-lived isotopes [14]. The appealing property of the classical approach was that a fairly comprehensive picture of *s* process could be drawn with very few free parameters and that these parameters are directly related to the physical conditions typical for the *s* process environment, i.e. neutron fluence, seed abundance, neutron density, and temperature. Moreover, it was found that reaction flow equilibrium has been achieved in mass regions of the main component between magic neutron numbers, where the characteristic product of cross section and *s* abundance, $\sigma N(A)$ is nearly constant. In spite of its schematic nature, the classical *s* process could be used to reproduce the solar *s* abundances within a few percent as illustrated in Figure 2.

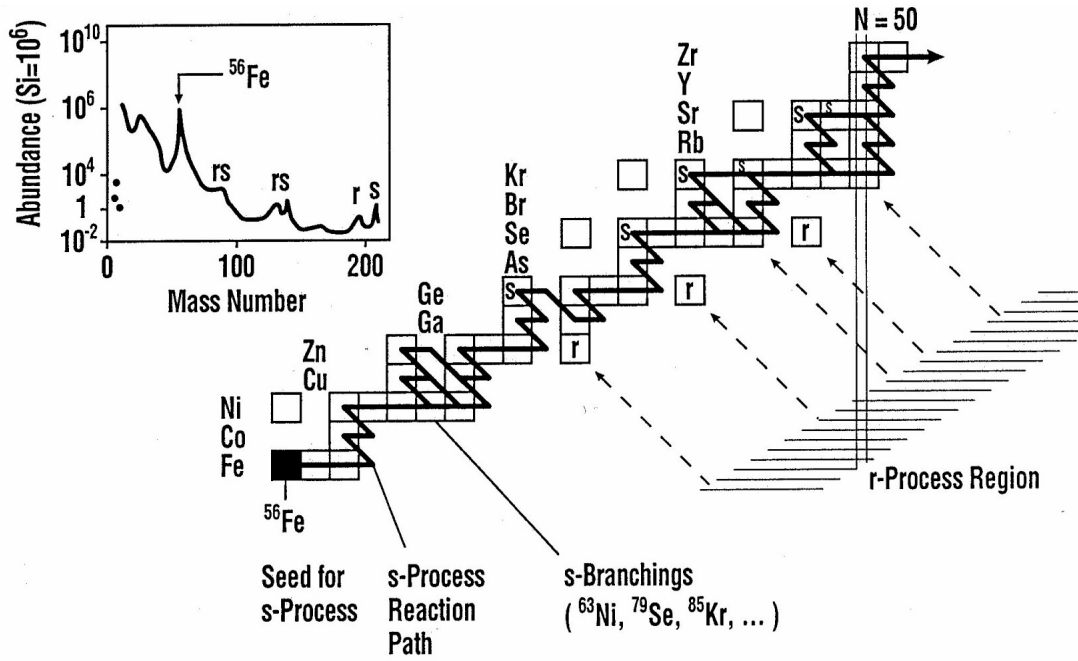


Figure 1. The formation processes of the elements between iron and the actinides. The neutron capture path of the *s* process follows the valley of stability and ends in the Pb/Bi region by α -recycling. Due to the much higher neutron densities, the *r*-process path is shifted to the far neutron-rich region, from where the reaction products decay back to stability. The solar abundances are essentially composed of contributions from both processes, except for the *s*-only and *r*-only isotopes, which are shielded by stable isobars against the *r*-process region or lie outside the *s*-process path, respectively. An additional minor component is ascribed to the *p* (or γ) process to describe the rare, stable proton-rich isotopes. The magic neutron number $N = 50$ is shown to indicate the strong impact of nuclear structure effects, which give rise to pronounced maxima in the observed abundance distribution as indicated in the inset.

Nevertheless, the more accurate cross section data became available, particularly around the bottle-neck isotopes with magic neutron numbers and in *s*-process branchings, the more inherent inconsistencies of the classical model came to light [15, 16], indicating the need for a more physical prescription based on stellar evolution [17]. This transition started with early models for stellar He burning by Weigert [18] and Schwarzschild and Härm [19], which were used by Sanders [20] to verify implicit *s*-process nucleosynthesis. The connection to the exponential distribution of neutron exposures postulated by the classical approach was ultimately provided by Ulrich [21] who showed that this feature follows naturally from the partial overlap of *s*-process zones in subsequent thermal instabilities during the He shell burning phase in low-mass asymptotic giant branch (AGB) stars. Consequently, the classical approach had been abandoned as a serious *s*-process model, but continued to serve as a convenient approximation in the mass regions between magic neutron numbers with constant σN_s products.

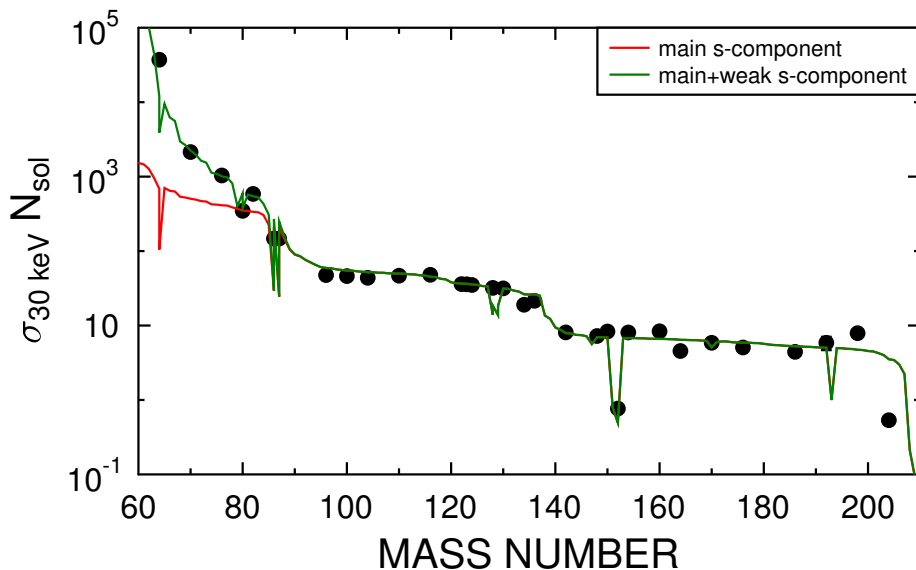


Figure 2. The characteristic product of cross section times s -process abundance plotted as a function of mass number. The thick solid line was obtained via the classical model for the main component, and the symbols denote the empirical products for the s -only nuclei. Some important branchings of the neutron capture chain are indicated as well. A second, weak component had to be assumed for explaining the higher s abundances between Fe and $A \approx 90$. Note that reaction flow equilibrium has only been achieved for the main component in mass regions between magic neutron numbers (where σN values are nearly constant).

The second half of the solar abundances above iron is contributed by the r process. In this case, the neutron densities are extremely high, resulting in neutron capture times much shorter than average β decay times. This implies that the reaction path is shifted into the neutron-rich region of the nuclide chart until the (n, γ) sequence is halted by inverse (γ, n) reactions by the hot photon bath. Contrary to the s process, where the abundances are dependent on the cross section values, the r abundances are determined by the β -decay half lives of these waiting points close to the neutron drip line.

As the consequence of the explosive supernova scenario suggested by B²FH, prescriptions of the r -process abundances were severely challenged by the fact that the required nuclear physics properties for the short-lived, neutron-rich nuclei forming the comprehensive reaction network far from stability were essentially unknown. This information includes β -decay rates and nuclear masses, neutron-induced and spontaneous fission rates, cross section data, and β -delayed neutron emission for several thousand nuclei. First attempts to reproduce the r -process abundances that had been inferred by subtraction of the s abundances from the solar values [11] started with a simplified static approximation, assuming constant neutron density and temperature ($n_n \geq 10^{20} \text{ cm}^{-3}$, $T \geq 10^9 \text{ K}$) during the explosion and neglecting neutron-induced

reactions during freeze-out [13]. Early dynamic r -process models were facing not only enormous computational problems, but had to deal with the many unknowns of the possible scenarios. In general, supernovae were preferred over supermassive objects and novae as potential r -process sites [22], but the relevant features of such explosions, i.e. the temperature and density profiles, the velocity distribution during and shortly after the explosion, and the initial seed composition, were too uncertain to draw a plausible picture of the r process by the end of the 1970ies [23].

As discussed by B²FH about 35 proton-rich isotopes cannot be produced by neutron captures, because they are shielded from the reaction networks of the s and r processes as shown in Figure 1. The initial idea that these isotopes were produced by proton capture (p process) in the hydrogen-rich envelope of massive stars during the supernova explosion [7] had to be abandoned because it led to unrealistic assumptions for densities, temperatures and timescales. In 1978, Woosley and Howard [24] suggested the shock-heated Ne/O shell in core-collapse supernovae as the site of the p process, where temperatures are high enough for modifying a preexisting seed distribution by a sequence of photo-disintegration reactions. Therefore, this approach is sometimes also referred to as γ process [25].

1.2. Solar abundances

The abundance distribution in the solar system has served as an important source of information for the nucleosynthesis concepts [7, 8, 9]. Following the pioneering work of Goldschmidt [26], detailed abundance tables have been reported by Suess and Urey [5] and were then continuously improved by the combination of meteoritic isotope abundances, essentially based on C1 chondrites, and of elemental abundances from spectroscopy of the solar photosphere. This series started with Cameron [27], Anders and Ebihara [28], Anders and Grevesse [29] and continued until now with compilations by Lodders [30], Grevesse et al. [31], and Lodders, Palme, Gail [32].

The distribution plotted in Figure 3 shows the solar system abundances as a function of mass number, which clearly exhibits the influence of nuclear effects characteristic of the various nucleosynthesis sites. The distribution is by far dominated by the primordial H and He abundances from the Big Bang followed by the rare elements Li, Be, and B. Because these are difficult to produce due to the stability gaps at $A = 5$ and 8, but are easily burnt in stars, the present abundances are essentially produced via spallation by energetic cosmic rays [33]. Stellar nucleosynthesis of heavier nuclei starts with ^{12}C and ^{16}O , the products of He burning, which were partly converted to ^{14}N by the CNO cycle in later stellar generations.

The light elements up to mass 50 are the result of charged-particle reactions during the advanced C, Ne, and O burning phases. This mass region is characterized by the enhancement of the more stable α nuclei and by the exponentially decreasing abundances due to the increase of the Coulomb barrier with atomic number. The last stage dominated by charged-particle reactions is Si burning, where densities and

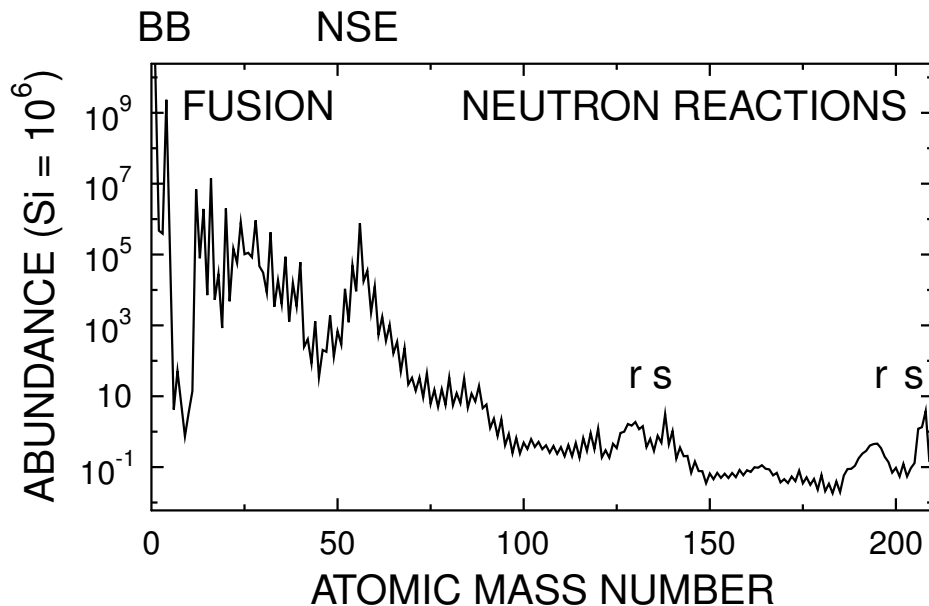


Figure 3. The isotopic abundance distribution in the solar system with indications for the main production processes (data from [32]). The *s* and *r* maxima are reflecting the effect of magic neutron numbers $N = 50, 82, 128$.

temperatures are high enough to reach nuclear statistical equilibrium. Under these extreme conditions only the most stable nuclei survive, leading to the distinct abundance peak around $A = 56$. Any further build-up of heavier elements were then provided by neutron capture reactions starting on these abundant isotopes, i.e. essentially on ^{56}Fe , as a seed as discussed in the following section.

2. Astrophysical models

2.1. The *s* process in asymptotic giant branch stars

In the advanced He burning stage of low-mass stars (1 to $5 M_{\odot}$, M_{\odot} being the mass of the sun) the stellar structure consists of an inert stellar core of carbon and oxygen, the products of He burning, surrounded by a narrow shell of about $10^{-2}M_{\odot}$ and a fully convective envelope as sketched in Figure 4. Within this thin layer, energy is produced in cycles, with several 10^4 years of H burning at the bottom of the convective envelope alternating with He burning episodes of about 50 years. This stage of evolution represents the scenario for the *s* process corresponding to the *main* component inferred by the classical *s* process [13].

During the H-burning period, He is produced from the bottom layers of the envelope. With the growing mass of the He intershell, the temperature in the intershell increases to the point, where He burning is triggered, resulting in a quasi-explosive thermal pulse (for details see Refs. [35, 34, 36, 37, 38]). Due to the sudden energy release,

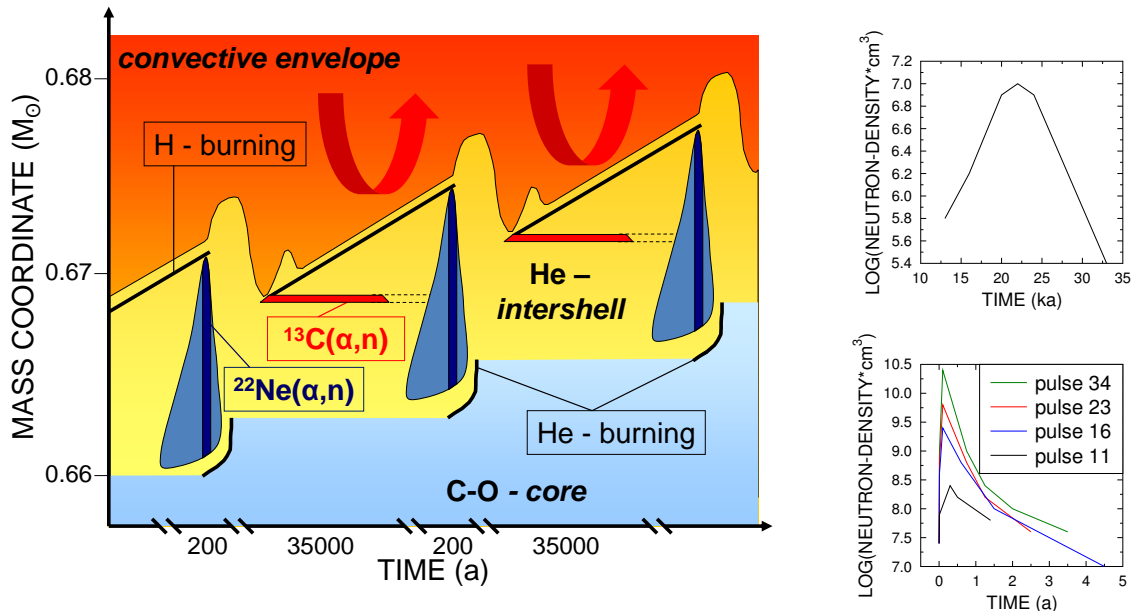


Figure 4. Schematic structure and evolution of AGB stars, showing recurrent H and He burning episodes with indications for the related s process sites (left). Right: Strength and time-dependence of the neutron density in thermally pulsing low-mass AGB stars contributed by (α, n) reactions on ^{13}C (top right) and ^{22}Ne (bottom right) [34]. Note that the efficiency of the latter increases with pulse number (11, 16, etc) due to the higher bottom temperature in later thermal pulses.

the radiative energy transport during H burning is completely converted to convection in the whole intershell, the envelope expands, the H shell burning is temporarily extinguished, and a large amount of ^{12}C is produced. The He shell burning continues radiatively for another few thousand years, before H shell burning starts again. In this way, thermal pulses might repeat 20 to 50 times depending on the initial stellar mass.

Significant neutron production and s processing starts with the third dredge-up (TDU) after a limited number of thermal pulses, when the C/O core mass reaches $\sim 0.6 M_{\odot}$ [37]. The term dredge-up refers to the unusual phases in the development of stars when surface material is convectively mixed deep into the interior of stars where the material has experienced nuclear reactions. As a result, freshly synthesized material is brought to the surface. If those episodes occur during the helium shell burning (AGB-phase), they are called third dredge-up, independent of how many pulses are actually participating in the process. TDU occurs when the H-shell is inactive after a thermal pulse and the convective envelope penetrates into the top region of the He-intershell, mixing newly synthesised ^{12}C and s -processed material to the surface and, at the same time, a few protons into the top layers of the He intershell.

After H burning resumes, these protons are captured by the abundant ^{12}C , thus initiating the sequence $^{12}\text{C}(p, \gamma)^{13}\text{N}(\beta^+ \nu)^{13}\text{C}$ in a thin region of the He-intershell, the so-called ^{13}C pocket [39]. Neutrons are released in the pocket under radiative conditions

by the $^{13}\text{C}(\alpha, n)^{16}\text{O}$ reaction at temperatures of $\sim 0.9 \times 10^8$ K [40]. At a neutron density of 10^6 to 10^7 cm^{-3} , about 95% of the neutron fluence in AGB stars is reached during this first stage of the s process because it is restricted to the thin ^{13}C pocket and lasts for about 10,000 years. In other words, the pocket is strongly enriched in s -process elements, before it is engulfed by the subsequent convective thermal pulse as indicated in Figure 4.

The mechanism for formation of the ^{13}C pocket is still a matter of debate, (for a discussion see Refs. [41, 42, 43, 44, 45, 36, 37]), but it is obvious that the H profile adopted in the pocket and the resulting amount of ^{13}C determines the final s -abundance distribution [46]. Consequently, the pocket is often parameterized to reproduce the observed s -process abundance patterns, e.g. the solar s distribution or s -process features found in presolar grains [47].

A second stage of the s process in AGB stars occurs during the maximum extension of the thermal pulse, when the temperature at the base of the convective zone exceeds 2.5×10^8 K. Under this condition, the $^{22}\text{Ne}(\alpha, n)^{25}\text{Mg}$ reaction is activated, maintaining a strong neutron burst for a few years. This neutron burst contributes only about 5% to the total neutron fluence in AGB stars, but its high neutron density of up to 10^{10} cm^{-3} , depending on the maximum temperature at the bottom of the thermal pulse, is instrumental for shaping the final abundance distribution, especially in the s -process branchings. The relative strengths and dynamics of the two neutron sources characterizing the s process in AGB stars are indicated in the right part of Figure 4 [40].

An important test of the current AGB model of the s process is again the comparison with the solar s abundances and with the isotope patterns of the s -process branchings. Based on the model described before excellent agreement had been demonstrated in Ref. [17] between solar s material and an average of models for 1.5 and 3 M_{\odot} AGB stars and was recently confirmed in [48] as illustrated in Figure 5. For the comparison, both distributions are normalised at the unbranched s -only nucleus ^{150}Sm . The AGB model obviously describes the set of s -only isotopes indicated by full circles to better than 10%. Different symbols were chosen for special s isotopes with non-negligible p contributions (^{128}Xe , ^{152}Gd , ^{164}Er , ^{180}Ta) and for the long-lived isotopes ^{176}Lu and ^{187}Os . The black full square corresponds to ^{208}Pb , which receives a contribution of about 50% by the strong s component produced in AGB stars of low metallicity [49, 50, 51]. Figure 5 illustrates that low-mass AGB stars contribute the main component to the solar s abundances from Sr to Pb/Bi, owing to the high neutron fluence in the ^{13}C pocket. The high fluence has two consequences. It leads to the depletion of the ^{56}Fe seed and of its progeny up to Sr at magic neutron number $N = 50$, and it is establishing a reaction flow equilibrium between magic neutron numbers characterized by $\sigma N_s \approx \text{constant}$. Accordingly, knowledge of a stellar cross section yields directly the corresponding s abundance of that particular isotope.

The reproduction of the main s component of the solar abundance distribution represents an impressive confirmation of the adopted s -process model that is

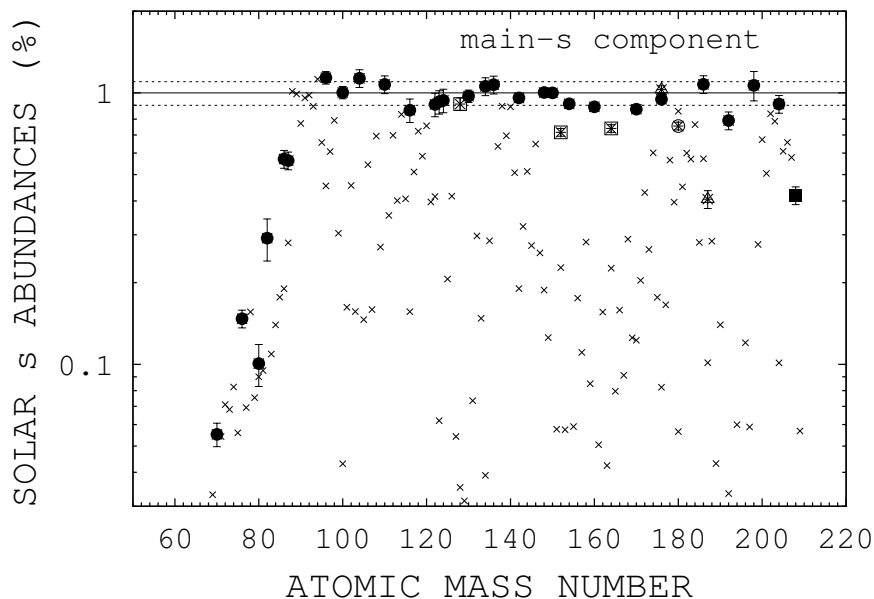


Figure 5. The main s component (in % of the solar abundances) normalized at the unbranched s -only isotope ^{150}Sm versus mass number [48]. The s -only isotopes between Sr and Pb/Bi (black circles) are reproduced to better than 10% except cases with sizable p components or the long-lived isotopes ^{176}Lu and ^{187}Os (open symbols) as well as the abundance of doubly magic ^{208}Pb (black square). Isotopes denoted by crosses are only partially produced by the s process (for details see text).

characterized by the complex interplay between the relative strengths and dynamics of the two neutron exposures operating in low-mass AGB stars, including the intricate abundance pattern of the various branchings along the s -process path. For a more complete account see Refs. [34, 52]. A comparison of low-mass AGB models computed with different evolutionary codes has been discussed by Lugaro *et al.* [53].

The maximum temperature during thermal pulses reaches about 3.5×10^8 K, leading to a substantial neutron production via the $^{22}\text{Ne}(\alpha, n)^{25}\text{Mg}$ reaction. However, the mass of the He intershell and the mixing efficiency of s processed material into the envelope are much smaller. Consequently, the predicted s -process abundance contributions are much lower than from low-mass AGB stars.

2.2. The s process in massive stars

As illustrated in Figure 5, the s process in low-mass AGB stars fails to reproduce the s abundances below $A \leq 90$. This gap is actually closed by the complementary weak s process taking place in massive stars with $M \geq 8M_{\odot}$, which explode as supernovae of type II. In massive stars, the s process is driven by the $^{22}\text{Ne}(\alpha, n)^{25}\text{Mg}$ reaction, first during convective core He burning at temperatures around 3×10^8 K and subsequently

during convective shell C burning at 10^9 K as discussed in Refs. [54, 55, 56, 57, 58].

The available ^{22}Ne is produced via the sequence of $^{14}\text{N}(\alpha, n)^{18}\text{F}(\beta, \nu)^{18}\text{O}(\alpha, n)^{22}\text{Ne}$ reactions, where ^{14}N originates from the CNO cycle in the previous H-burning phase. Consequently, this first part of the weak s -process in massive stars is secondary-like and decreases with metallicity. At He exhaustion in the core, not all the ^{22}Ne is consumed (e.g. [58]) and neutron production via $^{22}\text{Ne}(\alpha, n)^{25}\text{Mg}$ continues during shell C burning, where α particles are provided by the reaction channel $^{12}\text{C}(^{12}\text{C}, \alpha)^{20}\text{Ne}$ [59].

The chemical composition of the core up to a mass of $3.5M_{\odot}$ (for a star of $25M_{\odot}$) is modified during explosive nucleosynthesis in the supernova, which destroys any previous s -process signature. However, the ejecta still contain an important mass fraction of $2.5M_{\odot}$ that preserves the original s -process abundances produced by the hydrostatic nucleosynthesis phases of the presupernova evolution. This scenario was confirmed by post-processing models and full stellar models describing the evolution of massive stars up to the final burning phases and the SN explosion by the work of Raiteri *et al.* [60, 61, 62, 63] and a number of more recent investigations [64, 65, 66, 67, 68, 69].

In contrast to the main s -process component, the neutron fluence in the weak s process is too low for achieving reaction flow equilibrium (Figure 2). This has the important consequence that a particular neutron capture cross section not only determines the abundance of the respective isotope (as in case of the main component), but affects the abundances of all heavier isotopes as well [69]. This propagation effect is particularly critical for the abundant isotopes near the iron seed, where the effect was described first at the example of the $^{62}\text{Ni}(n, \gamma)^{63}\text{Ni}$ cross section [70, 71, 72]. An illustration is given in Figure 6 by changing the neutron capture cross section of ^{62}Ni under stellar conditions by factors of two. The problem with this cross section has triggered a whole series of experimental studies on ^{62}Ni [73, 74, 75, 76] as well as on other key reactions of the weak s process between Fe and Sr (see, e.g., [77, 78]). For a full account, see the recent update of the KADoNiS library [79].

The cumulated uncertainties of the propagation effect are affecting all isotopes of the weak s process, up to Kr and Sr, with possible, minor contributions to the Y and Zr abundances [69]. Once the neutron-capture cross sections of the isotopes between Fe and Sr will be determined with the required accuracy of 5%, the focus on the nuclear input for the weak s process will be on charged-particle reactions during He and C burning, which are difficult to determine (see, e.g., [67, 80]).

2.3. Explosive scenarios: r and p process

The second half of the heavy-element abundances in the solar distribution between Fe and the actinides, which are produced during the r process, can be inferred indirectly via the r -process residual method, i.e. by subtraction of the total s -process abundances, $N_r = N_{\odot} - N_s^{\text{weak}} - N_s^{\text{main}}$. Because the characteristic r -process abundance peaks fall in mass regions where the main s component reached reaction equilibrium, the classical s process is still a reasonable approximation and there is not much of a difference if the

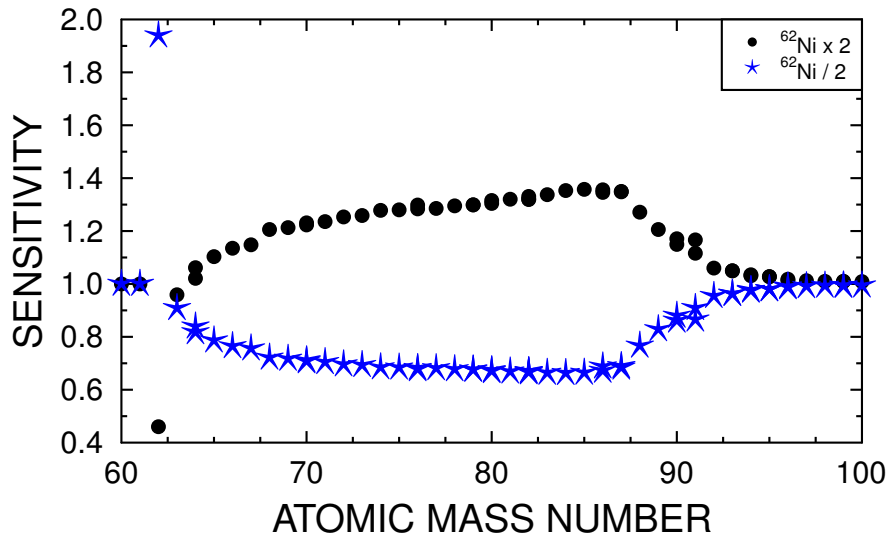


Figure 6. The sensitivity to the propagation effect of cross section uncertainties is illustrated at the example of ^{62}Ni . By changing the stellar neutron capture cross section of this single isotope by factors of two leads to drastic changes of the entire s abundances of the weak component.

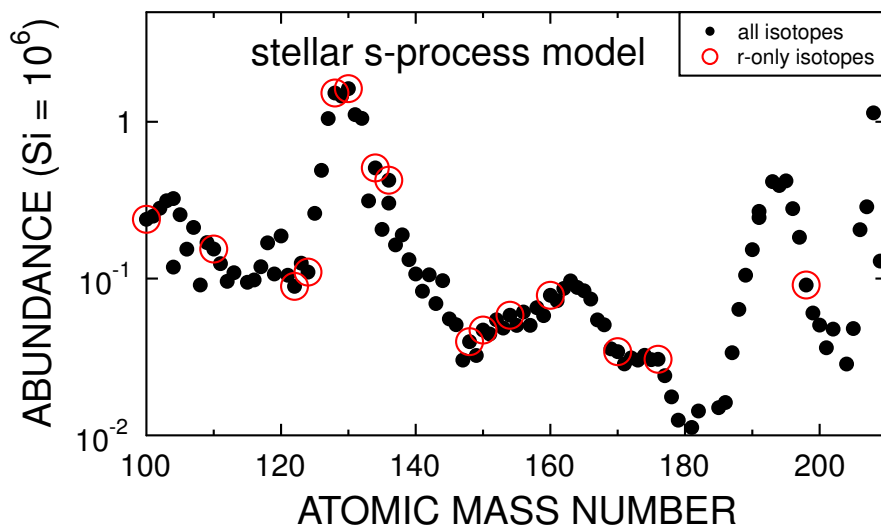


Figure 7. The r -process abundances (open squares) obtained via the r -process residual method, $N_r = N_\odot - N_s$, using the s -process abundances from Ref. [52]. The subset of r -only nuclei is marked by open circles. (N_i relative to $\text{Si}=10^6$).

s -process part is taken from the classical or from the stellar s -process prescription used for the distribution shown in Figure 7.

Apart from their relevance for testing the r -process models sketched below, the r -abundance distribution represents a key aspect for the composition of ultra-metal-poor stars [81, 82, 83, 84, 85, 86, 38], which turned out to agree almost perfectly with the scaled solar r component, thus indicating a unique, primary r process, at least for the elements heavier than Ba. Significant differences in the mass region below barium require, however, the assumption of additional r -process mechanisms. Accordingly, the quest for the astrophysical site(s) of the r process remains an open problem [87].

The broad r -process abundance peaks at $A = 80, 130, \text{ and } 195$ in Figure 3 are caused by accumulation of matter at closed neutron shells ($N = 50, 82, 126$), far from the stability valley on the neutron-rich side. The positions of these peaks suggest conditions that are realized in explosive environments with high neutron densities of $n_n > 10^{20} \text{ cm}^{-3}$ and temperatures of roughly 1 GK. The high neutron densities are driving the r -process path towards the neutron drip line until equilibrium between further neutron captures and reverse photodisintegration by the energetic photon bath is reached. This equilibrium is determined by the Saha equation in each isotopic chain and depends only on neutron density, neutron separation energy and temperature, completely independent of the respective (n, γ) cross sections.

Under these conditions, the reaction path runs along a path of constant neutron separation energy, where matter is accumulated at the so-called waiting points defined by $(n, \gamma) \Leftrightarrow (\gamma, n)$ equilibrium. The β -decay half-lives of the waiting points are determining the respective r abundances. Equivalent to the s process, the steady flow condition of the r process is expressed by a constant product of the beta decay rates λ times the abundances N_r , $\lambda(Z) \times N(Z) = \text{const}$. Therefore, the only nuclear physics properties needed to calculate r process abundances before freeze-out are β decay half lives and nuclear masses (or neutron separation energies). On the basis of experimental β -decay rates Kratz *et al.* [88, 89, 90] verified that steady flow equilibrium is indeed established in the r process. Recently, Wanajo showed that a "cold r process" scenario, operating at lower temperatures without establishing an $(n, \gamma) \Leftrightarrow (\gamma, n)$ equilibrium can also reproduce a solar-like r process abundance pattern [91].

While the waiting point concept has been applied mostly in static r -process calculations, models for the currently favored scenarios of neutrino-driven winds from nascent neutron stars [92, 93, 94], collapsar scenarios for long-duration gamma ray bursts (GRBs) [95], or neutron star mergers (e.g. [96]) follow the full comprehensive reaction network of the r process in much greater detail. Accordingly, so far all models are jeopardized by the lack of reliable nuclear physics data far from stability comprising the basic information on β -decay rates [97] and nuclear masses [98], but also neutrino interactions, β -delayed neutron emission, and β -delayed fission, not to speak of the intricacies of the respective astrophysical scenarios.

As long as neutron capture times are much shorter than β decays, the impact of neutron capture cross sections is negligible for the r -process networks. They are, however, relevant for the cold r process, where steady flow equilibrium is not achieved and neutron captures compete with β -decays [91], and also when in hot r process

scenarios the reaction flow falls out of equilibrium due to exhaustion of free neutrons.

In fact, it was shown that the onset of freeze-out is determined by the neutron capture rates [99]. During freeze-out they affect the final r process abundances, e.g. the exact position and width of the r process peaks as well as the smoothness of the abundance distribution in general [100, 101]. Neutron cross sections were shown to affect also the formation of the rare earth peak at $A \approx 160$ [101, 102, 103]. A number of key cross sections has been identified in sensitivity studies, e.g., in Refs. [104, 105]. Variation of the neutron capture rate by an order of magnitude can change the r abundances by up to 20%.

As a general rule, the neutron separation energy decreases with increasing neutron number for a given isotopic chain. Therefore the number of levels in the product nucleus, which can be populated directly or indirectly, is also decreasing. In the extreme case of a nucleus at the neutron drip line, where the neutron separation energy is close to zero, only the ground state can be populated in the product nucleus and the direct radiative capture (DRC) is strongly favoured over the resonant (compound nucleus) capture. This observation can be roughly summarized by: The more r -like the environment, the more dominates the DRC over the resonant captures [106, 107]. The crucial parameter, however, is not so much the separation energy, but the number of levels available in the product nucleus between ground state and neutron separation energy. If the level density is low -as for light or neutron-magic nuclei- the DRC might dominate even for stable nuclei.

Presently, it is still impossible to study r -process related neutron capture rates in direct measurements, because the relevant nuclei are way too short-lived. Instead, neutron capture cross sections can be obtained by indirect methods. This was demonstrated close to the doubly-magic waiting point ^{132}Sn by Kozub *et al.* [108], who investigated the single particle properties of ^{131}Sn by using the (d, p) reaction on ^{130}Sn in inverse kinematics. With this information, the DRC cross section could be calculated on the basis of experimental data. Next generation facilities will enable a number of new measurements on such critical nuclei. Apart from neutron capture rates, data on neutron induced fission play a major role for r -process cycling, and are essential to investigate the endpoint of the r process [109, 110]. More details on indirect methods can be found in Sec. 3.4.

Another nucleosynthesis mechanism, where neutron reactions are involved, is the p process, which is responsible for the 35 nuclei on the proton rich side of the stability valley, which are typically 10-1000 times smaller than the s and r process abundances. A promising site for the p process are the explosively burning Ne/O shells in the shock-heated envelopes of type II supernova explosions (e.g. [24, 111]) where a pre-existing s/r -seed distribution is eroded by photon-induced reactions at temperatures of 2-3 GK, resulting in a large network of (γ, n) , (n, γ) , (γ, p) , (γ, α) reactions and β -decays that extends a few mass units into the region of the unstable, proton-rich nuclei. A difficulty with this approach, however, are the abundances of the light p nuclei $^{92,94}\text{Mo}$ and $^{96,98}\text{Ru}$, which are exceptionally high and comparable to the neighboring s and r isotopes.

Therefore, separate production mechanisms have been proposed for these cases, such as the νp process in neutrino driven winds of SN II ejecta [112], the rp process in hot, proton rich matter that is accreted onto the surface of a neutron star [113, 114], and the ν -process [115]. However, Travaglio *et al.* showed recently that the p nuclei including the problematic cases $^{92,94}\text{Mo}$ and $^{96,98}\text{Ru}$ could be consistently produced in Type Ia supernovae explosions by treating a full p -process network coupled to a two-dimensional supernova scenario [116].

Although the p -process nucleosynthesis is mainly driven by photon-induced reactions, (n, p) reactions can push the nucleosynthesis path towards stability [117] and capture of free neutrons released in (γ, n) reactions may compete with the (γ, n) channel [118] and can affect the final p abundances or can modify even the seed abundances before onset of the p process [119].

Experimental possibilities for direct measurement of neutron reactions of relevance for the p process are facing similar but somewhat relaxed problems than in case of the r process, because the p -process network is much closer to the stability valley and comprises long-lived and even stable isotopes, particularly in the region of the light p nuclei. Examples of these cases have been identified in the sensitivity studies of Refs. [118, 117]. For the majority of the crucial competition points in the reaction network, however, the specific radioactivity remains a prohibitive obstacle. Therefore, the use of indirect methods is called for, similar to the situation on the r -process side mentioned before. The higher p -process temperatures of 2-3 GK requires that neutron-induced rates need to be known for $k_B T$ values of about 180-270 keV [118].

2.4. Galactic Chemical Evolution

The abundance distribution of the heavy isotopes must be considered as the result of all previous stellar generations that were polluting the interstellar medium before the formation of the Solar System. Presently, it appears that only the s process can be described with sufficient confidence to determine the cosmic s -process abundances in the framework of a general galactic chemical evolution (GCE) model.

Such an approach was reported by Travaglio *et al.* in a series of papers [120, 121, 49, 50, 51] using a model, in which the Galaxy is subdivided into three zones (halo, thick, and thin disk). With the s -process yields from a representative sample of AGB stars of different mass and metallicity, and accounting for their respective lifetimes, it was possible to follow the temporal enrichment of the s -process abundances in the interstellar medium [50, 51]. The resulting s -process distribution at the time when the solar system formed exhibits good agreement with the solar s abundances between barium and lead, including the solar ^{208}Pb abundance, which could be shown to originate mostly from low-metallicity AGB stars, thus providing a natural explanation for the strong s component. Below magic neutron number $N = 82$, however, the abundance distribution obtained by the GCE approach turned out to underproduce the solar s -process component between the Sr-Y-Zr region and barium by about 20 to 30% [52]. In

view of this deficit, an additional type of neutron-capture nucleosynthesis in the Galaxy, a light element primary process (LEPP) had been postulated [50], different from the s process in AGB stars and also different from the weak s -process in massive stars. The yet unknown origin of the LEPP is still a matter of debate [122, 123, 69, 124]. The parameters of the unknown process (e.g., the neutron density) have been discussed in [125] for reproducing the abundance patterns of HD 122563, a very metal-poor star showing a LEPP-type abundance pattern [126]. The clarification of the LEPP problem will certainly be furthered by a general improvement of the neutron capture cross section data between Sr and Ba.

Observational constraints of the galactic chemical evolution can be provided by spectroscopic observation of elemental abundances in stars of different metallicities, as they are representative for different ages of the galaxy. In this context, very old, ultra-metal-poor stars in the galactic halo attracted much interest, because their abundances are characterized by only few nucleosynthesis events. As mentioned before, these very old stars exhibit a solar-like r process distribution for the elements heavier than barium [127, 82, 85, 86], but also a clear deficit in the region below.

Under certain conditions, stars may experience convective-reactive nucleosynthesis episodes. It has been shown with hydrodynamic simulations that neutron densities in excess of 10^{15} cm^{-3} can be reached [128, 129], if unprocessed, H-rich material is convectively mixed with a He-burning zone. Under such conditions, which are between the s and r process, the reaction flow occurs a few mass units away from the valley of stability. These conditions are sometimes referred to as the i process (intermediate process). One of the most important rates, but extremely difficult to determine, is the neutron capture cross section of ^{135}I . While the $^{135}\text{I}(n, \gamma)$ cross section is not accessible by direct measurements because of the short half-life of about 6 h, the much improved production rates of radioactive isotopes at FAIR [130], however, offer the possibility to investigate the Coulomb dissociation cross section of ^{136}I . This reaction can then in turn be used to constrain the $^{135}\text{I}(n, \gamma)$ rate. In general, this method is suited for (n, γ) studies on neutron rich isotopes, because the decreasing neutron separation energies are favoring the DRC channel compared to the more complex compound mechanism as mentioned before (see also Sec. 3.4). The neutron separation energy of ^{136}I is only 3.8 MeV, since ^{136}I is neutron magic.

3. Neutron reactions

3.1. Definitions and current database

In stellar interiors, the plasma is considered to be in thermodynamic equilibrium. Hence, particles are quickly thermalized and their velocities v_x follow a Maxwell-Boltzmann distribution, which only depends on the mass m_x of the particle and on temperature T :

$$\phi(v_x)dv_x = 4\pi v_x^2 \left(\frac{m_x}{2\pi k_B T}\right)^{3/2} \exp\left(-\frac{m_x v_x^2}{2k_B T}\right) dv_x. \quad (1)$$

Here, $\phi(v_x)dv_x$ denotes the probability to find a particle with a velocity between v_x and $v_x + dv_x$, and k_B is the Boltzmann constant. For interacting nuclei X and Y the reaction rate per particle pair can then be written as:

$$\langle \sigma v \rangle = \int_0^\infty \phi(v)\sigma(v)v dv = 4\pi \left(\frac{\mu}{2\pi k_B T}\right)^{3/2} \int_0^\infty \sigma(v)v^3 \exp\left(-\frac{\mu v^2}{k_B T}\right) dv, \quad (2)$$

where v is the relative velocity between X and Y and $\mu = m_x m_y / (m_x + m_y)$ the reduced mass. Maxwellian average cross sections (MACS) are defined as the reaction rate scaled by the most probable velocity $v_T = \sqrt{k_B T / \mu}$ of the Maxwell-Boltzmann distribution:

$$\langle \sigma \rangle = \frac{\langle \sigma v \rangle}{v_T} = \frac{2}{\sqrt{\pi}} \frac{1}{(k_B T)^2} \int_0^\infty \sigma(E) E \exp\left(-\frac{E}{k_B T}\right) dE \quad (3)$$

According to the temperatures at the various s -process sites, MACS values need to be known for thermal energies $k_B T = 8$ to 90 keV. Therefore, neutron capture cross sections should be known up to several hundred keV, keeping in mind that the energy range above 400 keV contributes only about 1% to the thermal spectrum at $k_B T = 90$ keV. The effect on the MACS is even smaller because the cross sections are typically decreasing with increasing neutron energies. The situation is similar for r -process nucleosynthesis, where temperatures are typically ≤ 1 GK, corresponding to $k_B T$ values of at most 90 keV. The p process operates at higher temperatures, with $k_B T$ values up to 270 keV, requiring neutron cross sections up to at least 1 MeV.

In a first compilation by Macklin and Gibbons [10] MACS data were calculated from $k_B T = 5 - 90$ keV using the neutron capture information up to 1965. In the following decades, new and better experimental techniques became available, resulting in a wealth of new and more accurate measurements. Thanks to higher neutron fluxes and better detectors, measurements on many new isotopes were performed with significantly improved uncertainties, reaching a few percent in favorable cases. These data were collected in further MACS compilations by Käppeler *et al.* [131] and Bao *et al.* [132]. The latter became available online as the "Kadonis Astrophysical Database of Nucleosynthesis in Stars" (KADoNiS) and has been continuously updated to the present version v0.3 [79]. Recently, charged particle reaction rates for the astrophysical p process have been added as well [133].

Neutron cross sections for s -process studies are determined by two complementary methods. The time-of-flight (TOF) and the activation technique require both the production of a neutron beam. Because neutrons are unstable, it is not (yet) possible to perform experiments in inverse kinematics. Therefore, experiments are essentially limited to direct measurements of (n, γ) cross section on reasonably long-lived samples, but the potential for neutron capture studies via the inverse (γ, n) channel will be briefly touched as well.

3.2. Time-of-flight experiments

The TOF method enables cross section measurements as a function of neutron energy. Neutrons are produced quasi-simultaneously by a pulsed particle beam, thus allowing

one to determine the neutron flight time t from the production target to the sample where the reaction takes place. For a flight path L , the neutron energy is

$$E_n = m_n c^2 (\gamma - 1) \quad (4)$$

where m_n is the neutron mass and c the speed of light. The relativistic correction $\gamma = \left(\sqrt{1 - (L/t)^2/c^2}\right)^{-1}$ can usually be neglected in the neutron energy range of interest in nucleosynthesis studies and Eq. 4 reduces to

$$E_n = \frac{1}{2} m_n \left(\frac{L}{t}\right)^2. \quad (5)$$

The TOF method requires that the neutrons are produced at well defined times. This is achieved by irradiation of an appropriate neutron production target with a fast-pulsed beam from particle accelerators. The TOF spectrum measured at a certain distance from the target is sketched in Figure 8. The essential features are a sharp peak at $t = L/c$, the so-called γ -flash due to prompt photons produced by the impact of a particle pulse on the target, followed by a broad distribution of events when the neutrons arrive at the sample position, corresponding to the initial neutron energy spectrum.

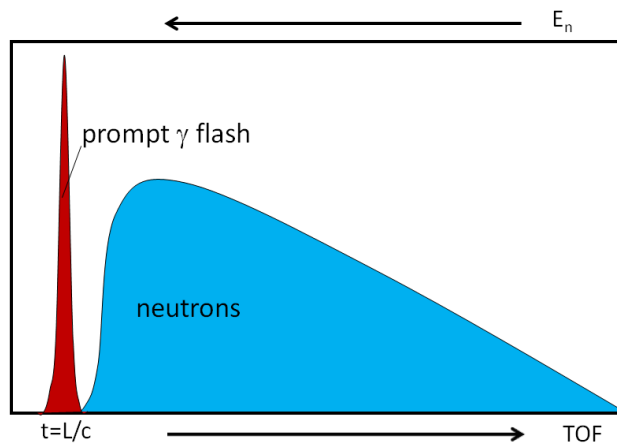


Figure 8. Schematic time-of-flight spectrum. The sharp peak at $t = L/c$ is caused by prompt photons produced by the impact of a particle pulse on the target. Neutrons reach the measurement station at later times and give rise to a broad distribution depending on their initial energies.

Neutron TOF facilities are mainly characterized by two features, the energy resolution ΔE_n and the flux ϕ . The neutron energy resolution is determined by the uncertainties of the flight path L and of the neutron flight time t :

$$\frac{\Delta E_n}{E_n} = 2\sqrt{\frac{\Delta t^2}{t^2} + \frac{\Delta L^2}{L^2}} \quad (6)$$

The neutron energy resolution can be improved by increasing the flight path, but only at the expense of the neutron flux, which scales with $1/L^2$. The ideal combination of energy resolution and neutron flux is, therefore, always an appropriate compromise. The energy resolution is affected by the Doppler broadening due to the thermal motion of the nuclei in the sample, by the pulse width of the particle beam used for neutron production, by the uncertainty of the flight path including the size of the production target, and by the energy resolution of the detector system.

The by far most important type of neutron reactions in astrophysics are neutron captures, which constitute the main production mechanism for the formation of the heavier chemical elements from iron to the actinides. The corresponding cross sections usually show a strong resonant structure, caused by the existence of excited levels in the compound nucleus. The excitation function for a reaction can accordingly be divided into three regions, the resonance region, where the experimental setup allows to identify individual resonances, the unresolved resonance region, where the average level spacing is still larger than the natural resonance widths, and the continuum region, where resonances start to overlap. The border between the first two regions is determined by the average level spacing and by the TOF resolution of the experiment.

Beside the resonant component related to the formation of a compound nucleus, there is also a small direct component to the cross section, which corresponds to events where the neutron is directly captured into the final state with concomitant emission of high-energy γ -rays. Because of its smooth dependence on neutron energy the direct component is not easily distinguishable from experimental background and, therefore, hard to identify in the resonance region. Direct capture is important for light as well as for the very neutron-rich, heavier nuclei involved in the r -process network, because in these cases the compound contributions are very small due to the low level densities in these nuclei.

In TOF measurements, capture cross sections are determined via the prompt γ -ray cascade emitted in the decay of the compound nucleus. The most common detection principles for measuring neutron capture cross sections are the use of total absorption calorimeters or total energy detection systems.

The total energy technique is based on a device with a γ -ray detection efficiency, ε_γ , proportional to γ energy, E_γ . Provided that the overall efficiency is low and that no more than one γ is detected per event, the efficiency for detecting a capture event becomes - on average - independent of cascade multiplicity and de-excitation pattern, but depends only on the excitation energy of the compound nucleus, i.e. the neutron separation energy. A detector with an intrinsic proportionality of E_γ and ε_γ was first developed by Moxon and Rae [134] by combining a γ -to-electron converter with a thin plastic scintillator. Because of this conversion, Moxon-Rae detectors are essentially insensitive to low-energy γ rays and were, therefore, used in TOF measurements on radioactive samples [135, 136]. The efficiency of Moxon-Rae detectors for capture events is typically less than a few percent.

Higher efficiencies of about 20% can be obtained by an extension of the Moxon-Rae principle originally proposed by Maier-Leibnitz [137, 138]. In these total energy detection systems the proportionality $E_\gamma - \varepsilon_\gamma$ is extrinsically realized by an *a posteriori* treatment of the recorded pulse-height. This Pulse Height Weighting technique is commonly used with liquid scintillation detectors about one liter in volume, small enough for the condition to detect only one γ per cascade. Present applications at neutron facilities n_TOF (Cern, Switzerland) and at GELINA (IRMM, Belgium) are using deuterated benzene (C_6D_6) as scintillator because of its low sensitivity to scattered neutrons. Initially, the background due to scattered neutrons had been underestimated, resulting in overestimated cross sections, particularly in cases with large scattering-to-capture ratios as pointed out by Koehler *et al.* [139] and Guber *et al.* [140, 141]. With an optimized design, an extremely low neutron sensitivity of $\varepsilon_n/\varepsilon_\gamma \approx 3 \times 10^{-5}$ has been obtained at n_TOF [142], which is especially important for light and intermediate-mass nuclei, where elastic scattering usually dominates the capture channel.

A total absorption calorimeter consists of a set of detectors arranged in 4π geometry, thus covering the maximum solid angle. Because the efficiency for a single γ -ray of the capture cascade is usually close to 100% in such arrays, capture events are characterized by signals corresponding essentially to the Q-value of the reaction. Provided good resolution in γ energy, gating on the Q-value represents, therefore, a possibility of significant background suppression.

Total absorption calorimeters exist at several TOF facilities. Most are using BaF_2 as scintillator material, which combines excellent timing properties, fairly good energy resolution, and low sensitivity to neutrons scattered in the sample. In fact, neutron scattering dominates the background in calorimeter-type detectors, because the keV-cross sections for scattering are typically 10 to 100 times larger than for neutron capture. In measurements at moderated neutron sources this background is usually reduced by an absorber surrounding the sample. Such a detector has been realized first at the Karlsruhe Van de Graaff accelerator [143]. This design, which consists of 42 crystals, is also used at the n_TOF facility at CERN [144], while a geometry with 160 crystals has been adopted for the DANCE detector at Los Alamos [145, 146]. In specific neutron spectra, e.g. in measurements with the Karlsruhe array, where the maximum neutron energy was about 200 keV, scattered neutrons can be partially discriminated via TOF between sample and scintillators, because the capture γ rays reach the detector before the scattered neutrons [143]. There are also 4π arrays made of NaI crystals [147, 148], but in the astrophysically important keV region these detectors are suffering from the background induced by scattered neutrons, which are easily captured in the iodine of the scintillator.

At white neutron sources, the highest neutron energy for which the neutron capture cross section can be determined is limited by the recovery time of the detectors after the γ flash. While the accessible neutron energy range is practically not restricted for C_6D_6 detectors, BaF_2 arrays are more sensitive, depending on the respective neutron source. At n_TOF, for example, the BaF_2 calorimeter can be used only up to few tens of keV,

whereas there are no strong limitations at Los Alamos. Independent of the detection system used, measurements at higher neutron energies are increasingly difficult because the (n, γ) cross section decreases with neutron energy, while at the same time competing reaction channels, e.g. inelastic neutron scattering, are becoming stronger. Nevertheless, present techniques are covering the entire energy range of astrophysical relevance up to about 500 keV with sufficient accuracy.

Apart from neutron capture, there are also other neutron-induced reactions of relevance for stellar nucleosynthesis. While neutron-induced fission of the very short-lived isotopes involved in the r process is presently inaccessible to experiments, the impact of (n, p) and (n, α) reactions can dominate over neutron capture, especially in the mass region below Fe. Examples are the neutron poison reaction $^{14}\text{N}(n, p)^{14}\text{C}$ [149, 150] and the recycling reaction $^{33}\text{S}(n, \alpha)^{30}\text{Si}$ impeding the s production of ^{36}S [151, 152].

Ionization chambers are popular for cross section measurements of reactions with charged particles (cp) in the exit channel. These detectors have the advantage that they are rather insensitive to neutrons and can be operated directly inside the neutron beam, thus covering a large solid angle. Different designs have been used for astrophysical cross section measurements at various TOF facilities, for example Frisch-gridded chambers in (n, cp) measurements at Karlsruhe and GELINA, (e.g. [151] and [153], respectively) or a compensated chamber at ORELA [154]. Among the current gas detectors the Microbulk Micromegas type [155] is a fairly new development, which is based on the MicroMegas principle [156] and has the advantage of fast timing and the capability for spatial resolution [157]. The very low material budget of this type allows one to share the same neutron beam line with another experiment by operating the detector in parasitic mode, in parallel to other experiments. Its low sensitivity to the γ flash and its comparatively high gain make the detector particularly suited for measurements of (n, cp) cross sections, where the ejectile energies are typically a few MeV only.

Fast ionization chambers are frequently used in fission cross sections measurements, where background problems are relaxed because of the comparably high Q-values (e.g. Ref. [158]). More detailed information on the fission process can be obtained with parallel plate avalanche counters [159], for example on the fission fragment angular distribution [160]. Further advantages of these detectors are excellent time and spatial resolution and their practically negligible response to the γ flash.

Compared to gas detectors, silicon detectors are superior in energy resolution and better suited for particle identification in TOF experiments. They are, however, sensitive to neutron damage, and are, therefore, usually operated outside the neutron beam. Silicon detectors have been successfully used in measurements of (n, p) and (n, α) cross sections (see, e.g. [150, 161]) as well as for monitoring the neutron flux [162]. Recently, a chemical vapor deposited (CVD) diamond detector has been developed at n_TOF for measurements of (n, cp) cross sections [163]. Diamond detectors are radiation hard and can be operated almost background-free even directly in the neutron beam. However, their energy resolution does not reach that of silicon detectors.

3.3. The activation method

To obtain stellar cross sections from an activation experiment, the neutron spectrum should ideally correspond to the perfectly thermal spectrum at the respective *s*-process site. By serendipity, the ${}^7\text{Li}(p, n){}^7\text{Be}$ reaction, which represents the most prolific neutron source at low energy accelerators fulfills this requirement almost perfectly [164, 165, 166]. Adjusting the proton energy at $E_p = 1912$ keV, 30 keV above the reaction threshold, yields a neutron spectrum with an energy dependence close to

$$\Phi_n(E) = E \exp\left(-\frac{E}{k_B T}\right) \quad (7)$$

as required in the MACS definition of Eq. 3 for the case of $k_B T = 25$ keV almost perfectly mimicking the situation during He shell flashes in AGB stars (Sec. 2.1).

This quasi-stellar neutron source is ideally suited for the determination MACS data for a number reasons:

(i) The experimental setup is rather simple. Because the proton energy is just above the reaction threshold, all neutrons are emitted in a forward cone with an opening angle of 120 degrees. Because the accelerator can be operated in direct mode and the sample can be placed directly at the neutron production target, the neutron flux in activation measurements is orders of magnitude higher than can be achieved in TOF experiments. The higher flux results in an enormous gain in sensitivity, thus allowing for measurements of very small cross sections and/or on very small samples. (ii) Samples can be used in natural isotopic composition or even as compounds, because the reaction products are detected off-line in a low-background environment via their characteristic decay modes. In favorable cases this allows one to measure the cross sections of several isotopes at the same time or to determine the partial cross sections for feeding isomeric states, an aspect that is important for the reaction flow in some of the branchings. (iii) Backgrounds are strongly reduced. For example, the effect of scattered neutrons and the ambient γ background, which is immanent to TOF experiments, are completely eliminated. Sample-related effects due to multiple scattering and self-shielding can be avoided by using very small samples. In general, the comparably short measurement times allows one to study systematic uncertainties experimentally by repeated activations under modified conditions.

However, the method is limited to cases where neutron capture leads to an unstable isotope with a half-life longer than about a second. Moreover, the quasi-stellar spectrum is not exactly thermal and the respective corrections (which are usually very small though) require the knowledge of the energy dependence of the cross sections. A more severe problem results from the fact that quasi-stellar spectra can only be produced for very few temperatures. Apart from the ${}^7\text{Li}(p, n){}^7\text{Be}$ reaction for $k_B T = 25$ keV, other possibilities are provided by (p, n) reactions on ${}^{18}\text{O}$ for $k_B T = 5$ keV [167] and ${}^3\text{H}$ for $k_B T = 52$ keV [168], both with significantly reduced intensities. This means that the MACS determined via activation may have to be inter- or extrapolated to cover the full range of *s*-process temperatures. Unless the energy-dependence of the cross section is

well defined experimentally, this procedure may cause sizable uncertainties.

In view of its attractive features, the activation technique has been extensively used at the Karlsruhe Van de Graaff. Across the nuclear chart, MACS measurements have been carried out on 120 isotopes according to the KADoNiS compilation [79]. Typically, the induced activity can be measured via the γ emission of the product nucleus, which implies favorable signal-to-background ratios and the unambiguous identification of the reaction products. The excellent selectivity achieved in this way can often be used to study more than one reaction in a single irradiation. A prominent example is Xe, where five cross sections can be measured simultaneously [169]. If suited compounds are used for the sample material, cross sections of all constituents can be determined as in case of RbBr, where MACS data for all four stable isotopes could be obtained [78].

The technique allows very good accuracy as demonstrated by the 1.4% uncertainty claimed for the MACS of ^{197}Au [164]. Examples for the unique sensitivity are measurements of very small cross sections at the μb -level, e.g. on ^{15}N with a MACS-value of only $6 \mu\text{b}$ for $k_B T = 25 \text{ keV}$. Similarly small cross sections were obtained for ^{14}C [170] and ^{18}O [171]. Both are particular, because the short half-lives of the reaction products required the use of a fast cyclic activation scheme [172].

The excellent sensitivity of the activation method was mandatory for measurements on very small samples of the unstable branch-point isotopes ^{135}Cs [173], ^{147}Pm [174], ^{155}Eu [175], ^{163}Ho [176], ^{171}Tm [177], and ^{182}Hf [178]. Among these cases, the 28 ng of ^{147}Pm represent the smallest sample ever used in an (n, γ) cross section measurement in the keV region. In dealing with MACS measurements on unstable isotopes, the possibility for using sample sizes of a few μg or even less is particularly crucial, because these materials are hard to produce. Another important aspect in using small radioactive samples is that it allows one to keep the radiation hazards and the related backgrounds at a manageable level. Here, ^{60}Fe deserves special mentioning as the measurement of this MACS is complicated by the small (n, γ) cross section as well as by the difficulty in obtaining a suitable sample [179, 180].

While fast cyclic activation is called for in case of short-lived reaction products, long-lived product nuclei are more difficult to deal with, in particular if the induced activities are near or below the detection limit. If decay counting of the reaction product becomes too difficult, the reaction products can be directly counted using Accelerator Mass Spectrometry (AMS), an ultra-sensitive technique to measure isotopic ratios as small as 10^{-16} . AMS was first been applied for cross section measurements by Paul et al. for the $^{25}\text{Mg}(p, n)^{26}\text{Al}$ reaction [181]. A prominent example for an (n, γ) reaction is the case of ^{62}Ni , where the product nucleus ^{63}Ni has not only a half-life of 101 years, but decays without any γ emission and a very low β -endpoint energy of 70 keV [73, 182]. Meanwhile, AMS has been applied successfully for MACS measurements on ^9Be and ^{13}C [183], ^{14}N [184], ^{40}Ca [185], ^{54}Fe [186], ^{58}Ni [187], and ^{78}Se [188].

3.4. Indirect measurements

Depending on the reaction type the corresponding indirect approaches are very different. Within this review, only the techniques important for neutron studies, i.e. inverse reactions and surrogate reactions, will be discussed.

The Coulomb dissociation (CD) method can be used to determine the desired cross section of the reaction $A(n, \gamma)B$ via the inverse reaction $B(\gamma, n)A$ by applying the detailed balance theorem. It has been shown that this method can be successfully applied, if the structure of the involved nuclei is not too complicated, as in the case of the reaction $^{14}\text{C}(n, \gamma)^{15}\text{C}$ [170]. If the reaction product B is short-lived, the CD method can be applied at radioactive beam facilities [189, 190].

Limitations of the CD method are (i) the applicability of this method to heavier nuclei close to the valley of stability due to the high level density in the compound nucleus, and (ii) because the resolution of current facilities of ≥ 100 keV is not sufficient to constrain the astrophysically relevant cross section.

Restriction (i) is alleviated in r -process studies, because the level density is rapidly decreasing as the Q -values drops towards the neutron drip line. This implies that fewer levels are important, and the part of the capture cross section, which can be constrained via the inverse reaction, increases. Restriction (ii) motivated the development of improved experimental approaches such as NeuLAND@FAIR, which aims for an energy resolution of better than 50 keV [191].

If the product is stable or very long-lived, also real photons can be used to study $B(\gamma, n)A$ reactions [192, 193]. In principle the same restrictions apply as for the Coulomb dissociation method.

Surrogate reactions have been successfully used for obtaining neutron-induced fission cross sections [194]. This approach is using a charged particle reaction for producing the same compound system as in the neutron reaction of interest. In this way, a short-lived target isotope can be replaced by a stable or longer-lived target. For neutron capture reactions, however, the method is challenged because the compound nucleus that is produced in the surrogate reaction is characterized by a spin-parity distribution that can be very different from the spin-parity distribution of the compound nucleus occurring in the direct (n, γ) reaction [195, 196].

4. Facilities and achievements

4.1. White neutron sources

Commonly, the term "white" refers to accelerator-based neutron sources, where an initially hard neutron spectrum region is softened by a moderator for producing a continuous neutron spectrum covering the energy range from the high production energies in the MeV to GeV region down to thermal values.

The highest neutron yields are obtained in spallation reactions of high-energy beams. As spallation neutrons are very energetic, a moderator near the neutron

production target is needed to shift the spectrum to the lower neutron energies of astrophysical interest. TOF facilities at spallation neutron sources are presently operating at CERN [197, 198, 199], at Los Alamos National Laboratory [200] and at J-PARC [201].

At n_TOF, intense 20 GeV pulses of 7×10^{12} protons are producing about 2×10^{15} neutrons per pulse in a massive lead target, corresponding to 300 neutrons per incident proton. The target is cooled with water, which acts also as moderator. The resulting neutron spectrum ranges from thermal energies of 25 meV to a few GeV. The flight path of 185 m and the proton pulse width of 7 ns, offer a very good energy resolution. During the approximately 10 years of successful operation, a large number of (n, γ) reactions of stable nuclei on the s process path has been studied with C_6D_6 scintillation detectors (Sec. 3.2), i.e. isotopes of Fe and Ni [202], Zr [203, 204, 205], La [206], Au [207], Pb [208], and Bi [209] as well as the potential neutron poison isotopes of magnesium [210]. Particular projects are the capture cross sections of $^{186,187,188}\text{Os}$ for determining the age of the universe via the Re/Os clock [211, 212, 213] and the cross sections of the unstable branch point isotopes ^{63}Ni ($t_{1/2} = 101.5$ yr) [214] and ^{151}Sm ($t_{1/2} = 93$ yr) [215, 216]. In addition, the (n, α) cross section of the long-lived isotope ^{59}Ni ($t_{1/2} = 76$ kyr) has recently been determined with a special CVD diamond mosaic-detector [163].

At the Los Alamos Neutron Science Center (LANSCE), a proton beam with an energy of 800 MeV reacts with a W target. The total neutron yield at the target station is smaller than at n_TOF, but the time-integrated neutron flux at the sample position is on average about 20 times higher than at n_TOF due to a shorter flight path of 20 m and a higher repetition rate of 20 Hz (vs. 0.4 Hz at n_TOF). On the other hand, the proton pulse width of 120 ns is limiting the energy resolution in the keV region, and as a consequence, only average cross sections can be determined above about 10 keV. Measurements of astrophysical interest started with (n, p) cross sections [150, 217, 218] and have been later extended to neutron capture data for $^{62,63}\text{Ni}$ [75, 219] and $^{147,151}\text{Sm}$ [220, 221].

At the Material and Life science experimental facility at J-PARC in Japan, an intense, pulsed neutron beam is produced via spallation of 3 GeV protons on a mercury target. Besides the focus on material and life sciences, one beam line at a distance of 22 m from the target is dedicated to neutron cross section measurements, using the Accurate Neutron-Nucleus Reaction Measurement Instrument (ANNRI). ANNRI consists of 2 detection setups, a 4π Ge detector array and a NaI(Tl) spectrometer. Neutron fluxes at the current beam power of 120 kW are about a factor then higher than at the 20 m station at LANSCE. The final beam power of 1 MW will boost the flux by another factor of 10. Due to the long pulse width of $1 \mu\text{s}$ the neutron energy resolution is deteriorating already at several hundred eV. Current efforts concentrate on neutron capture measurements on minor actinides and long-lived fission products, e.g. $^{244,246}\text{Cm}$ [222].

Electron accelerators have been used for neutron production via bremsstrahlung-induced (γ, f) and (γ, n) reactions by irradiation of high- Z targets with pulsed electron

beams. A prominent example was the Oak Ridge Electron Linear Accelerator (ORELA) [223], where important experimental techniques have been developed [138, 224] and where most of the initial MACS data for s -process studies have been determined in numerous measurements by Macklin and collaborators (see, e.g., [225, 226, 227, 228], including first studies on unstable isotopes [229, 230, 231, 232]. After an update of the experimental setup, astrophysics at ORELA was resumed by Koehler *et al.* with (n, γ) and (n, α) measurements on isotopes of Sr, Mo, Ba, Sm, and Pt [233, 234, 235, 236, 237, 238].

When ORELA was closed in 2012, GELINA at Geel/Belgium [239, 240] remained the only electron-driven, moderated facility for neutron studies in the energy regime of the s process. The accelerator delivers a 140 MeV electron beam with a pulse width of 1 ns onto a rotating U target, and the water-moderated neutron spectra from 25 meV up to 20 MeV can be accessed at 10 flight paths from 10 to 400 m. The astrophysics activities are essentially carried by visiting groups and are devoted to (n, γ) cross sections of isotopes on the s process path, e.g., Si [241], Kr [242], Nd [243], and Ba/Pb [244]. As a complement to the (n, γ) studies, (n, α) and (n, p) cross sections were measured for ^{17}O [245], ^{26}Al [153] and for ^{36}Cl [246], respectively.

At the ELBE accelerator at Dresden-Rossendorf a 40 MeV electron beam on an unmoderated liquid metal target is used to operate a very compact neutron source characterized by a remarkably high TOF resolution [247]. Applications in astrophysics are hampered, however, by the hard neutron spectrum that is concentrated in the energy range from 0.2 to 10 MeV with an intensity maximum around 1 MeV, too high for most astrophysical (n, γ) measurements.

About a factor of 10^4 higher neutron fluxes than at conventional TOF facilities can be produced with lead slowing down spectrometers (LSDS), however, at the expense of neutron energy resolution, which is $> 30\%$ (FWHM). An LSDS consists of a pulsed neutron source surrounded by high purity lead blocks, typically 1 m^3 in volume. Neutrons get trapped in the lead for several hundreds of microseconds and are slowed down by inelastic and elastic scattering. Losses due to neutron capture on Pb are very small, because the capture cross sections are orders of magnitude smaller than for scattering. At LSDS facilities cross section measurements can be performed on minute samples of a few tens of ng, and are, therefore, well suited for measurements on short-lived isotopes and/or samples of high specific activity. The first LSDS was built in the 1950ies [248], and the concept has been revived, e.g. at CERN [249], Los Alamos [250], and KURRI [251]. Neutron cross section measurements with LSDS spectrometers have been mainly used for fission and capture cross section measurements for reactor applications (see e.g. [252, 253]), but have potential for measurements on s process branching points as well.

4.2. Low-energy accelerators

Neutron production via (p, n) reactions at low-energy electrostatic accelerators was the initial source of information on stellar cross sections [10]. When electron linacs came

into routine operation in the late 1960ies most experimental activities were attracted by the higher flux and better energy resolution of the new neutron sources. About 15 years later, however, the specific advantages of low-energy machines led to a revival, particularly for applications in astrophysics.

Fast pulsed electrostatic accelerators are important because they are complementary to white neutron sources due to a combination of unique features, i.e. the possibility to tailor the neutron spectrum, low backgrounds, and competitive flux at sufficient TOF resolution. Neutron spectra can be restricted to the immediate region of interest for *s*-process applications by the proper choice of the proton energy and the thickness of the neutron production target. For the example of the ${}^7\text{Li}(p, n){}^7\text{Be}$ reaction, which has been used in most cases because it represents the most prolific (*p, n*) source, neutrons in the energy range from a few to 220 keV are produced by bombarding layers of metallic Li or LiF typically 10 to 30 μm in thickness. With proton beams 30 and 100 keV above the reaction threshold at 1881 keV, continuous neutron spectra with maximum energies of 100 and 225 keV are obtained, where the first choice offers a significantly better signal to background ratio at lower neutron energies. The neutron production target consists only of a thin Li layer on a comparably thin backing without any moderator, thus allowing for very short flight paths down to a few centimeters. In this way, neutron intensities at the position of the sample are becoming comparable to those of white neutron sources in spite of the lower neutron production yields and higher repetition rates [254]. And, not to forget, low-energy accelerators bear the option for activation measurements in quasi-stellar neutron spectra (Sec. 3.3).

Thanks to these options, particularly the Karlsruhe Van de Graaff has been extensively used for astrophysics studies. In the optimized TOF mode, typical beam parameters were an average proton current of 2 μA at a repetition rate of 250 kHz, and a pulse width of 0.7 ns, perfectly matching the 0.5 ns time resolution of the 4π BaF₂ array that was originally developed for (*n, γ*) studies at this accelerator [143]. With flight paths around 80 cm, a flux similar to that of electron linacs could be obtained at a TOF resolution of 1.2 ns/m, fully adequate for the determination of MACS data in the temperature range of the various *s*-process scenarios.

The Karlsruhe activities are covering the mass range of the entire *s*-process path from carbon to bismuth. Particularly fruitful was the setup with the 4π BaF₂ detector, which has been extensively used for determining an accurate and comprehensive set of MACS data in the mass range of the main component from Nb to Ta. In this program, emphasis was put on the *s*-only isotopes of Sn [255], Te [256], Xe [257], Ba [258], Sm [259], Gd [260], and Lu [261] to characterize important *s*-process branchings as well as to establish a grid for normalization of the $N_s\sigma$ distribution via the MACS data of ${}^{110}\text{Cd}$ [262], ${}^{142}\text{Nd}$ [16], and ${}^{150}\text{Sm}$ [259]. The full potential of the 4π BaF₂ array has been demonstrated in the MACS measurement on Nature's rarest stable isotope ${}^{180}\text{Ta}^{\text{m}}$ [263, 264]. Although the total world supply of that isotope could be obtained, the sample consisted of only 150 mg Ta with a modest enrichment in ${}^{180}\text{Ta}^{\text{m}}$ of 5.5%. In this case, the option of using the Q-value difference was crucial for discriminating

events of the dominant impurity ^{181}Ta .

An important feature of low-energy accelerators is the possibility of tailoring the neutron spectra by the choice of neutron source reaction, proton energy, and thickness of the neutron production target [265]. Special examples are the kinematic collimation of the neutron beam providing the possibility to reduce neutron flight paths to a few centimeters with an enormous increase of the flux at the sample position (e.g. [136, 266]). This option allowed also to produce a narrow energy beam for a measurement of the (n, n') cross section [212] for complementing the nuclear physics input for dating the Universe by means of the Re/Os chronometry [213].

The flexibility of low-energy accelerators has also been used for experiments with unique sensitivity to the DRC channel at TIT Tokyo [267], which provided the MACS data for the very abundant isotopes ^{12}C [268], ^{13}C [269], and ^{16}O [270], which are important neutron poisons for the s process in spite of their minute (n, γ) cross sections.

To complete this section, it is worth mentioning the potential of reactor filtered neutron beams, which are produced by means of sharp interference dips on the low-energy side of broad scattering resonances. A first astrophysically motivated measurement that was reported using the 24 ± 2 keV spectrum obtained with an iron filter [271] already showed that this method has the advantage of very clean, well-defined spectra covering a relatively narrow energy range. A unique set of neutron filters has been installed at the Kyiv reactor, providing more than 10 neutron lines in the energy range from thermal to several hundred keV with intensities of $10^6 - 10^8 \text{ cm}^{-2}\text{s}^{-1}$ [272, 273]. Apart from activation measurements for normalization of uncertain differential (n, γ) cross sections, filtered neutron beams are important for measurements of elastic and inelastic scattering cross sections, which are needed for the quantitative assessment of the influence of thermally populated excited states on the MACS. The uncertainty of the respective correction, the so-called stellar enhancement factor (Sec. 4.3), can be significantly reduced provided that all reaction channels are constrained by experimental data as demonstrated for the important case of ^{187}Os [213]. In that study, a quasi-monoenergetic neutron beam was produced via the $^7\text{Li}(p, n)$ reaction [212], but with much lower intensity and less resolution than at Kyiv, for example.

4.3. Role of Theory

Typical reaction networks for explosive nucleosynthesis contain about 2000 mostly unstable isotopes connected by more than 20000 reactions. These numbers underline the importance of theoretical predictions for the astrophysical rates of all these reactions. Whenever possible, the theoretical predictions are supported, guided, and constrained by experimental data, but for the foreseeable future, by far the largest part of this information will depend on models suited for global predictions of nuclear properties. The current half-life limit for direct measurements of neutron capture rates is a few years. With the new facilities on the horizon (Sec. 5.1), this limit will be reduced to about 100

days [274], still not sufficiently low to contribute to our understanding of the r process, even of the freeze-out phase [100]. The same holds true for the i process [128, 129] with the neutron capture cross section of ^{135}I ($t_{1/2} = 6$ h) as an important example (Sec. 2.4). The continuous attempts for constructing such global approaches are reflected in huge databases, which are often available online, e.g. by works of Rauscher *et al.* [275, 276, 277] and Goriely [278], or by the data obtained with the Talys code [279].

Even if experimental cross section data are available, very often these data are not fully commensurable with the energy regime of the stellar situation. In such cases, cross sections obtained with theoretical models can be normalized to the available experimental data. If the uncertainty of the energy dependence of the calculated cross section is small, this method provides a safe extrapolation to the relevant stellar energies from the measured energies. This approach was applied to a number of isotopes, where the cross section has been determined only by activation in a quasi-stellar spectrum corresponding to $k_B T = 25$ keV (for examples see [132]).

Cross section data from laboratory experiments are subject to corrections for temperature effects, because low-lying excited nuclear states are thermally populated in the hot environment of the interior of stars. As their cross sections generally exceed the respective ground state values, the corresponding correction is often denoted as stellar enhancement factor (SEF). The SEF corrections depend critically on the excitation energies of the first few nuclear states and are important if the lowest excited states occur within an energy window corresponding to three to four times the thermal energy of the stellar environment. Under the conditions of the s -process component in AGB stars, this affects states below about 100 keV, but at the higher temperatures in massive stars this window is extended to 300 keV or higher. The problem of the SEF corrections and their uncertainties has been recently addressed in detail by Rauscher *et al.* [275, 276].

On a laboratory scale, the excited states decay quasi instantly via γ -emission and are, therefore, out of reach for direct measurements. The only chance in the foreseeable future might be to use the NIF facility at LLNL [280], where laser-heated fusion plasmas can be produced with temperatures above 10 keV, but presently the determination of SEF corrections remains subject to statistical model calculations.

The input for such calculations, however, can be derived from experimental data on the ground state cross section complemented by the statistical properties of neutron resonances and by the cross sections for the competing elastic and inelastic scattering channels as demonstrated in case of ^{187}Os , where the first excited state occurs already at 9.8 keV [213]. A similar approach has also been used for the MACS calculation of the branch point nucleus ^{192}Ir by adjusting the parameters used in the Talys code on the basis of experimental cross section data for the Ir and Pt isotopes [238]. Also indirect methods can be useful to constrain the relevant model parameters. For example, time-reversed experiments can provide the ratio for populating excited states and ground state, thus contributing to the calculation of excited state cross sections.

4.4. Stellar decay rates

In addition to the potential temperature-dependence of the neutron capture rates [132], analyses of *s*-process branchings are facing severe theoretical problems in determining the weak interaction properties. Although all rates for β -decay and electron capture (EC) of relevance in the *s* process are known under terrestrial conditions, contributions of thermally populated excited states as well as atomic effects in the strongly ionized stellar plasma can dramatically modify the laboratory values [281]. The calculated β rates in stellar environments are subject to nuclear uncertainties, which remain difficult to estimate, because the related uncertainties depend strongly on the experimentally unknown decay properties of excited states.

Under stellar conditions, ground state and low-lying excited states are in thermal equilibrium. The combined β -decay rates of the involved states determine, therefore, the β -decay probability of each species. So far, almost all stellar decay rates have been inferred in a semi-empirical way by Takahashi and Yokoi [281] on the basis of decay systematics derived from analogue states in neighboring nuclei. In order to illustrate the effect of the remaining nuclear uncertainties, these calculations have been iterated by modifying the unknown transition rates by an error value of $\log ft = \pm 0.5$ [282]. For typical *s*-process conditions (temperature 3×10^8 K and electron density $N_e = 10^{27} \text{ cm}^{-3}$), the final rates differed by a maximum factor of three, but the individual variation depends strongly on the excitation energies and decay patterns of the individual excited states.

In case of isomeric excited states with sufficiently long half-lives one may attempt to determine the weak-decay rate experimentally. An example is the decay of ^{79}Se , where the 96-keV isomer ($t_{1/2} = 3.9$ min) could be sufficiently populated for measuring its β -decay half life of about 5 d [283], leading to a drastic reduction of the terrestrial half life of 3×10^5 yr to a few years under *s*-process conditions. Apart from isomeric states, β decay properties of excited states have not been measured in the laboratory yet. In addition, stellar decays are affected by modes, which are energetically not possible on earth, i.e. EC from the continuum or bound β decay. These effects, which may alter the decay rates by orders of magnitude [281], represent a permanent experimental challenge.

If the β -decay Q-value is small, the correspondingly long terrestrial half-lives of such nuclei can be dramatically shortened in a hot stellar plasma, where the degree of ionization is high or even complete. This opens the possibility for bound-state β decay, where the electrons are emitted directly into empty atomic orbits. The mechanism of bound-state β -decay has been successfully verified by following the decay of fully stripped ions in the Experimental Storage Ring at GSI/Darmstadt. Half-lives for bound-state β decay have been measured for ^{163}Dy [284], which is stable in its neutral state, and for ^{187}Re [285], which is important for the Re/Os cosmic chronometer [213]. Additional examples are ^{205}Hg and ^{207}Tl [286].

For the theoretical calculations of stellar rates, Gamow-Teller strength distributions $B(\text{GT})$ for low lying states are needed [287, 288, 289]. Charge-exchange reactions, e.g.

(p, n) , provide access to the strength of these transitions via the proportionality between the cross sections at low momentum transfer q close to 0° and $B(GT)$,

$$\frac{d\sigma^{CE}}{d\Omega}(q=0) = \hat{\sigma}_{GT}(q=0)B(GT), \quad (8)$$

where $\hat{\sigma}_{GT}(q=0)$ is the unit cross section for GT transitions at $q=0$ [290]. As shown in Ref. [291] this kind of information can also be obtained via $(d, {}^2\text{He})$ reactions, which can be studied with high-resolution magnetic spectrometers. In order to access GT distributions for unstable nuclei, experiments could be carried out in inverse kinematics with radioactive ion beams.

5. Current developments and new opportunities

Current efforts in laboratory developments are focused on facilities with higher fluxes and on detectors with high efficiencies and low inherent backgrounds. These features are crucial for studies of unstable isotopes, where often sample sizes are limited due to restricted availability or a high specific activity, but are likewise important for accurate measurements of small cross sections.

5.1. New facilities

Currently, some facilities are under construction, which will yield neutron fluxes up to two orders of magnitude higher than currently available. This large increase is either based on the installation of a shorter flight path, like at n_TOF EAR-2, or on using an innovative new accelerator design to run small scale accelerators with unprecedented beam intensities (for example the projects FRANZ and SARAF).

The EAR-2 project [198, 199] is an upgrade of the n_TOF facility at CERN [197, 292] by complementing the existing experimental area at 185 m (EAR-1) by a new experimental area at a shorter flight path of 20 m. Figure 9 shows a sketch of the EAR-2 project, which is expected to start operation the summer of 2014.

The new flight path will be installed vertically at an angle of 90 degrees with respect to the 185 m flight path serving the existing experimental area (Sec. 4.1). Charged particles are removed from the neutron beam by a permanent magnet, and the neutron beam is shaped by collimators for optimized conditions with respect to capture and fission experiments. Compared to EAR-1, the main advantages of EAR-2 are higher average and instantaneous neutron fluxes (by factors of 25 and 250, respectively). In addition, the γ flash is reduced, because γ rays and ultra-relativistic particles produced in the target are predominantly emitted in the direction of the proton beam. The performance of the new flight path is presently optimized by detailed simulations and will be studied in detail during an extended commissioning campaign.

A different approach that will be well suited for both, time-of-flight and activation measurements, is pursued at Goethe University Frankfurt, Germany [293, 294, 295, 296]. The Frankfurt Neutron Source of the Stern Gerlach Zentrum (FRANZ), which is

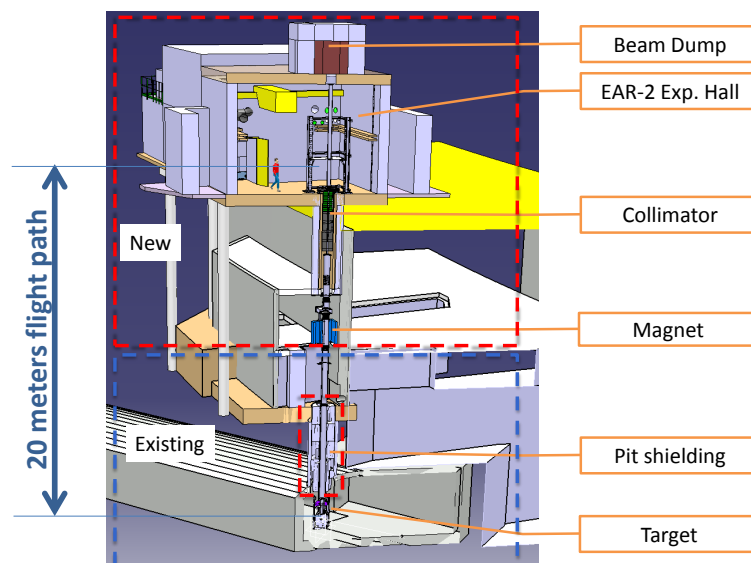


Figure 9. Sketch of the second experimental area (EAR-2) currently under construction at n_TOF/CERN. EAR-2 will be placed at 90 degrees with respect to the CERN-PS proton beam. The shorter flight path of 20 m results in a flux which is 20-30 times higher than at the 185 m measurement station EAR-1. (© n_TOF@CERN)

currently under construction, is based on a high intensity proton accelerator using the ${}^7\text{Li}(p, n)$ reaction for neutron production in the energy range up to 500 keV. The layout of the FRANZ facility is shown in Figure 10.

The proton beam of 100-250 mA DC, produced in a volume type ion source, is first accelerated to 2.0 MeV in a radiofrequency quadrupole section (RFQ) coupled to an interdigital H-type (IH) structure. The final proton beam with an energy between 1.8 and 2.2 MeV and an energy resolution of 20 keV is obtained by a drift tube cavity downstream of the IH part. Nominal proton currents will be limited to 20 mA DC, resulting in a 1000 times higher neutron flux than what was available for TOF measurements at Karlsruhe. For activation measurements, the total neutron yield will be 10^{12} neutrons per second. For TOF measurements, the proton beam is compressed to bunches of 1 ns, using a chopper system at the entrance of the RFQ with a repetition rate up to 250 kHz and a Mobley-type bunch compressor. In this configuration, the total neutron yield will be 2×10^{11} neutrons per second. As the experimental conditions are very similar, most of the equipment was transferred after the shutdown of the Karlsruhe Van de Graaff, including the 4π BaF₂ array mentioned in Sec. 3.2.

Because the amount of sample material can be reduced by the gain in flux, TOF measurements at FRANZ appear to be feasible already with samples of 10^{14} atoms. This number represents a break-through with respect to the production of unstable samples, because beam intensities of the order of 10^{10} to 10^{12} s^{-1} are expected at future Rare

Isotope Facilities such as FRIB [297], RIKEN [298], or FAIR [299].

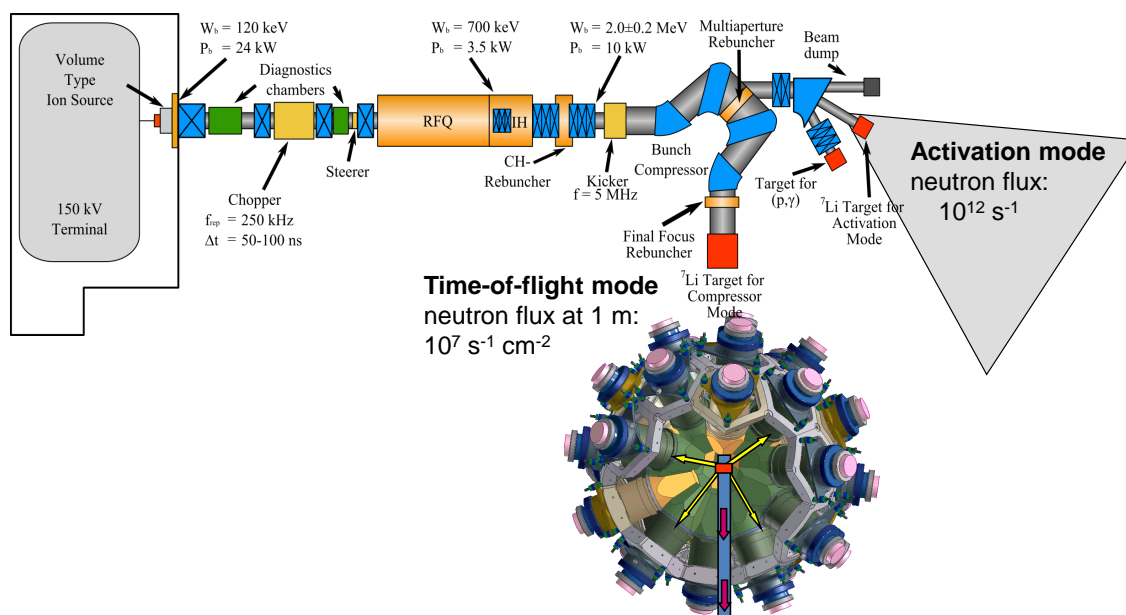


Figure 10. Sketch of the neutron facility FRANZ, currently under construction at Goethe University Frankfurt/Germany

A low-energy approach is also being realized at the Soreq Applied Research Accelerator Facility SARAF (Soreq NRC, Israel) [300, 301], where deuteron and proton beams of 2 mA and energies up to 40 MeV are obtained with a superconducting linac. Recently, first neutrons were successfully produced via the ${}^7\text{Li}(p, n)$ reaction by means of an innovative windowless Liquid-Lithium Target (LiLiT) [301]. For technical reasons astrophysics experiments at this facility will be concentrated on the activation method.

A similar concept has been adopted for planning the LEgnaro NeutrOn Source LENOS. Proton beams of initially 5 MeV energy and 50 mA current will be degraded to achieve an energy distribution, which can be used to produce different neutron spectra of quasi-Maxwellian shape via the ${}^7\text{Li}(p, n)$ reaction [302]. There is also potential to measure cross sections of radioactive species by combining the neutron beam with radioactive beams provided by the future SPES project [303].

Intense neutron sources with low-energy particle beams are also under development for medical applications. Projects for cancer treatment by boron neutron capture therapy (BNCT), e.g. at Birmingham [304], are using the ${}^7\text{Li}(p, n)$ reaction and are also working in the energy regime of astrophysical interest.

Table 1. Comparison of integrated neutron flux between 10 and 100 keV and energy resolution of operating and future TOF facilities.

Facility	ϕ_n (10^4 s $^{-1}$ cm $^{-2}$)	ϕ_n (pulse $^{-1}$ cm $^{-2}$)	$\Delta E/E$ (in units of 10^{-3})
n_TOF EAR-1 (185 m)	0.4	1×10^4	1-2
LANSCCE (20 m)	13	7×10^3	8 - 26
GELINA(30 m)	1.4	18	1.3
FZK (1 m)	1	0.01	3 - 10
n_TOF EAR-2 (20 m)	8	2×10^5	10-20
FRANZ (1 m)	600	6	3 - 10

The performance of some existing and future TOF facilities is compared in Table 1 in terms of neutron flux and resolution. The flux values (in units of cm $^{-2}$ s $^{-1}$ and cm $^{-2}$ pulse $^{-1}$) represent integrals over the neutron energy range from 10 to 100 keV, which are most important for astrophysical applications. Among existing facilities, LANSCCE is offering the highest neutron flux per cm 2 s, however, with limited neutron energy resolution due to the long pulse width of the primary proton beam. Comparable fluxes are obtained at GELINA (30 m station), n_TOF (EAR-1 at 185 m), and previously at Karlsruhe (80 cm). In terms of neutron flux per pulse, n_TOF has the highest intensity, resulting in very good signal to background conditions, which are of advantage for measurements on radioactive samples. At GELINA, shorter flight paths of 10 m are also available, thus offering higher neutron flux, but at the expense of neutron energy resolution.

The neutron flux at the future FRANZ facility was calculated to be factors of 60 – 600 higher than at existing installations, using the code PINO [265]. Monte Carlo simulations of the neutron flux at the future n_TOF EAR-2 suggest that the neutron flux per time unit will increase by a factor of about 25 with respect to the existing n_TOF EAR-1, making the flux comparable to LANSCCE. The instantaneous neutron flux, however, is expected to increase by a factor of 250, a key advantage of the CERN facility. The neutron flux over the full energy range covered by these TOF facilities is compared in Figure 11.

Note that activations at existing low-energy accelerators and particularly at the future FRANZ facility can be performed in quasi-stellar neutron fields that are still orders of magnitude more intense than achievable even in the most advanced TOF installations.

5.2. Detectors

In general, neutron capture events are detected via the prompt γ -ray cascades. The best signature of these cascades is the total energy that is defined by the Q-value of the reaction. Depending on the level structure of the product nucleus, the energy distribution of the emitted γ -rays can be very broad, which means the possibility of

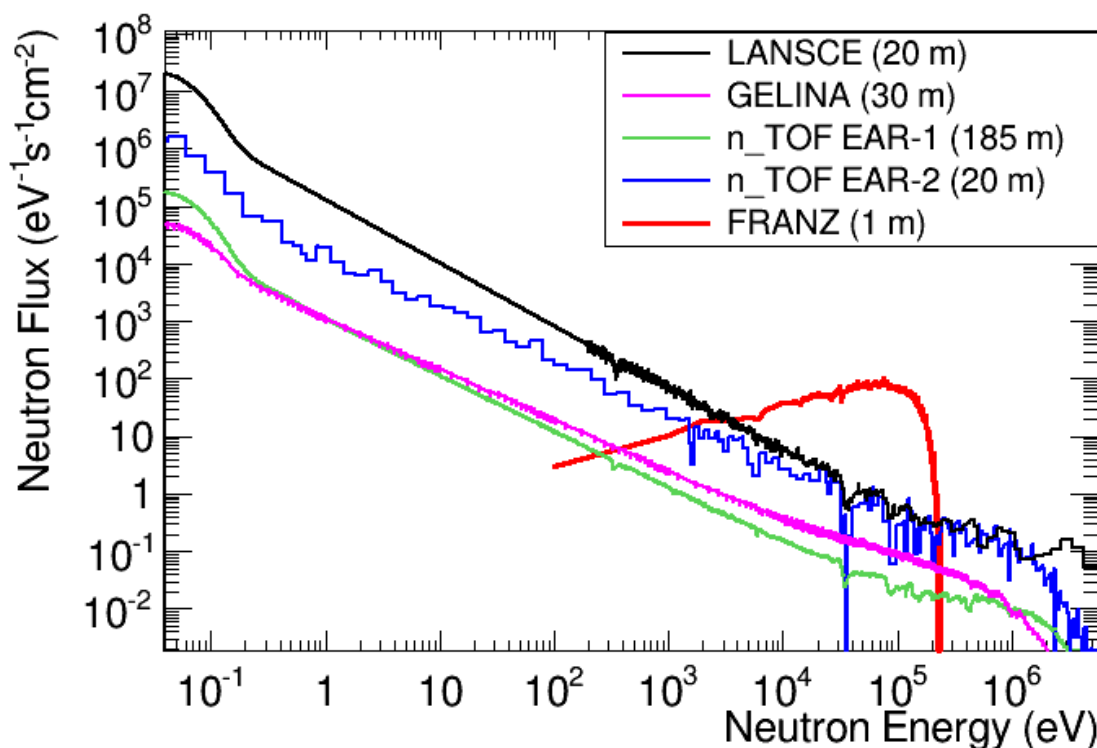


Figure 11. Comparison of the neutron flux at existing and future facilities as listed in Table 1.

background discrimination based on the energy of single γ -rays is not restricted by the energy resolution of the detector. Therefore, most approaches sacrifice energy resolution for detection efficiency or neutron sensitivity.

The sensitivity to neutrons is extremely important, since the neutron scattering cross section in the keV-regime can be several orders of magnitude higher than the neutron capture cross section under investigation. Accordingly, the detectors are exposed to sample-scattered neutrons, which may cause significant backgrounds. The most successful technique for suppressing such backgrounds is based on liquid C_6D_6 scintillation detectors, which can be optimized for extremely low neutron sensitivity [142]. Advanced detectors of this type are used on a regular basis, in particular if isotopes with very small (n, γ) cross sections are under investigation [210].

Important progress in this field may come from a new concept based on composite detectors of low efficiency. Using the directional information obtained via the Compton effect the idea aims for a strong reduction of the ambient background from neutron interactions in the detectors and room walls [305].

An important and broadly used alternative approach is the calorimetric detection of all emitted γ -rays. This technique, where capture events are discriminated against backgrounds via the specific Q-value of the investigated sample, requires 4π detectors of high-Z materials with sufficient resolution in γ energy and detection efficiencies near

100%. The first array suited for the keV region was the Karlsruhe 4π BaF₂ detector [143] (Sec. 3.2). BaF₂, which is among the scintillators with the lowest response to neutrons and exhibits also excellent timing properties (Table 2), became also the material of choice [145] for other 4π calorimeters [146, 144].

Meanwhile, more scintillators can be produced in sufficiently large volumes. Some attractive alternatives are compared with established detector materials in Table 2 with respect to density or absorption length, wavelength of the scintillation light, signal intensity given by the number of photons produced per γ -ray energy, and decay time. The entries in the last column correspond to a quality factor for the sensitivity to scattered neutrons.

Among the new scintillators, Ce doped LaBr₃ represents an interesting alternative, because of the superior energy resolution indicated by the large number of photons per keV γ energy. Whether the background reduction obtained with a narrow Q-value window compensates the effect of the rather high neutron sensitivity may well depend on the specific experimental situation. From the examples listed in Table 2, high-efficiency scintillators such as BaF₂ represent a balanced compromise between a modest energy resolution and low neutron sensitivity. In that respect LaCl₃ might offer a promising unexplored solution. Extreme cases are C₆D₆ detectors, which combine an extremely low neutron sensitivity with poor resolution in γ -energy, whereas the excellent energy resolution of Ge-detectors is to be paid with a comparably high sensitivity to scattered neutrons. The latter choice, which has been adopted for the ANNRI array at J-PARC/Japan [306], provides additional information on the decay patterns of the capture cascades, however.

Another important aspect is the decay time of the scintillation light. Most time-of-flight facilities suffer from an intense γ -flash caused by the impact of the particle beam on the neutron production target that results in a high energy deposition in the detectors at very short flight times (see Figure 8). Particularly at short flight paths, the dead time caused by the γ flash impedes or even prevents the registration of neutron-induced events at later times. The longer the decay time of the detector material and the shorter the flight path, the lower the maximum energy for which capture events can be observed. As soon as this energy limit falls below 10 keV, the setup is of limited value for astrophysical purposes.

The prompt detection of charged particles requires very thin samples and is, therefore, challenging in terms of the observed count rate. The detector is usually more massive than the sample, thus requiring the possibility of discriminating reactions in the sample and in the detector. One approach is to place the detectors outside the neutron beam sacrificing solid angle coverage. Fast silicon detectors of different sizes and granularities are suited for this purpose, i.e. for cross section measurements of (n, α) reactions [307] and for neutron beam monitors using the ${}^6\text{Li}(n, \alpha)$ reaction [162]. Alternatively, efficiencies of nearly 100% are obtained with highly transparent detectors, which can be placed directly inside the neutron beam. Most common are gas detectors, e.g. ionization chambers, which have been operated in the single

Table 2. Characteristics of some scintillator materials.

Scintillator	Density (g/cm ³)	Abs. length ^a cm	Wave- length (nm)	Photons per keV	Decay time (ns)	Quality ^b s _γ /s _n
C ₆ D ₆	0.954	14	425	≈10	2.8	80000
C ₆ F ₆	1.61	10.1	430	10	3.3	610
BaF ₂ ^c	4.88	3.5	220; 310	1.8; 10	0.6; 630	300
Bi ₄ Ge ₃ O ₁₂ ^c	7.13	2.1	480	0.7; 7.5	60; 300	520
NaI(Tl)	3.67	4.6	415	38	250	23
CsI(Na)	4.51	3.8	420	41	630	22
CeF ₃ ^c	6.16	2.7	300; 340	0.2; 4.3	3; 27	740
LaCl ₃ (Ce)	3.85	4.3	350	49	28	430
LaBr ₃ (Ce)	5.08	3.4	380	63	16	27
Lu _{1.8} Y ₂ SiO ₅ (Ce)	7.1	2.2	420	32	41	29

^aThickness of detector material needed to reduce the intensity of 1 MeV γ -rays by $1/e$.

^bRatio of total photon absorption cross section for 1 MeV γ -rays and Maxwellian averaged neutron capture cross section of the scintillator material at 30 keV.

^cMaterial with two components in scintillation light.

Frisch-gridded version [153, 308] or with reduced background in the compensated mode [154].

More recently, MicroMegas detectors [156, 157] were successfully used at CERN. Advantages of this detector are its very low background, fast timing, spatial resolution, and a sufficiently low noise level for application in (n, α) measurements. In fission studies, parallel plate avalanche counters (PPAC) turned out to be extremely insensitive to neutrons and γ -rays. This feature is crucial in the neutron energy range above 100 MeV, where other detectors are overwhelmed by the γ flash [309, 160]. Diamond detectors became another option for in-beam detection of charged particles with good time and energy resolution. Because they are only available in rather small sizes so far, a composite diamond detector was recently used for an (n, α) cross-section measurement by the n_TOF collaboration at CERN [163].

In activation measurements the induced activities of the product nuclei are measured off-line (Sec. 3.3), using techniques according to the half-life and the decay mode of the reaction product. In most cases, HPGe detectors are applied, ideally with segmented configurations, e.g. Clover type detectors. In this way, a high efficiency can be combined with a reduced load per detector, an important aspect if the sample itself is radioactive. The power of this approach has been demonstrated at the example of the $^{147}\text{Pm}(n, \gamma)$ reaction [174]. This measurement could be performed on only 10^{14} atoms by using the high efficiency of a two-Clover setup in close geometry and the coincidence

option for detecting γ cascades in the decay of ^{148}Pm .

Special examples are reactions, in which the product nuclei decay either without γ emission or are long-lived isotopes so that the induced activities fall below the detection limit. The latter cases can be studied via accelerator mass spectrometry, still maintaining the excellent sensitivity of the activation technique as discussed in Sec. 3.3. Examples from the first category, however, suffer from significantly reduced sensitivity, because the required detection of the decay electrons implies the use of very thin samples to avoid excessive absorption losses [310].

5.3. Advanced concepts

While existing techniques are sufficient to study most neutron reactions on stable isotopes with the required accuracy, neutron capture data for radioactive nuclei, which are of key importance in advance nucleosynthesis models (Sec. 2), are presenting a number of experimental challenges. An inherent difficulty in measurements on radioactive samples results from the radiation emitted by the sample itself, thus imposing stringent limits on the sample size that can be handled in such experiments. Other major problems are the production of sufficiently clean and isotopically pure samples and the coordination of production and experiment in order to minimize the ingrowth of the daughter nuclei.

An obvious solution for dealing with small samples is to increase the neutron flux [274], either by increasing the neutron production rate or by decreasing the distance from the neutron production target. As spallation sources are operating with a fixed primary beam, a higher flux can be obtained by reducing the flight path, e.g. at the n_TOF facility, but at the expense of a correspondingly reduced resolution in neutron energy. Actual developments of new low-energy accelerators, e.g. the FRANZ project, offer the possibility for increasing the flux by both options, higher intensity of the primary beam as well as a reduction in flight path. For example, if FRANZ would be operated with a flight path of 10 cm instead of 1 m with a nominal time resolution of 1 ns, the neutron-energy resolution is still comparable to the one at DANCE (Table 1) but the neutron flux at the sample position would be about $10^9 \text{ cm}^{-2}\text{s}^{-1}$, orders of magnitude higher than in any other TOF facility.

A completely different approach is to investigate neutron-induced reactions in inverse kinematics [311]. This requires a beam of radioactive ions cycling in a storage ring with 100 AkeV or less and a neutron target. Radioactive ions close to stability can be produced with high intensities using ISOL-techniques and storage rings for low beam energies, which require extremely high vacuum, are under construction, e.g. the CRYRING at GSI/FAIR [312] or the CSR at MPK/Heidelberg [313]. The neutron target could be either a reactor coupled with the storage ring to obtain an interaction zone near the core [311] or a bottle of ultra-cold neutrons. The scheme of such a setup is sketched in Fig. 12.

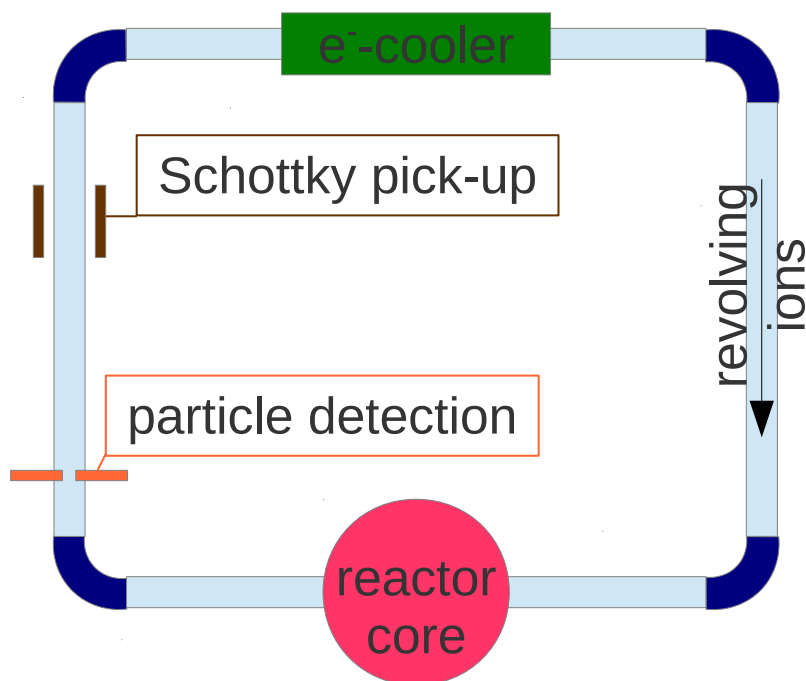


Figure 12. Proposal for (n, γ) measurements on short-lived isotopes [311]. The main components are an ion storage ring with beam lines and focusing elements (light blue), dipole magnets (dark blue) and electron cooler (green). The ring is coupled to a thermal reactor with an interaction region near the core (red). Capture events are identified by particle detectors outside the nominal orbit (orange) and/or by Schottky pick-up electrodes (brown).

6. Status and requests

6.1. Compilations of stellar (n, γ) cross sections

In 1971, the first comprehensive collection of recommended MACS values for $k_B T = 30$ keV by Allen *et al.* [11] listed 130 experimental cross sections with typical uncertainties between 10 and 25%. To provide a full set of data for the early pioneering studies of the s -process, the experimental results were complemented by 109 semi-empirical values estimated from cross section trends derived from neighboring nuclei.

The next compilation published in 1987 [314] was prepared again for MACS values at a single thermal energy of $k_B T = 30$ keV, according to the needs of the classical approach for a scenario of constant temperature and neutron density [13]. A major achievement, however, was the significant improvement of the accuracy, which was reaching the 1 - 2% level for a number of important s -process isotopes.

When the classical approach had been challenged by refined stellar models with a range of s -process conditions, from He shell burning in thermally pulsing low mass AGB stars [315, 316] to shell C burning in massive stars [60, 61] and with (α, n) reactions on ^{13}C and ^{22}Ne as the main neutron sources, the compilations had to be extended to provide MACS data for thermal energies between 5 and 100 keV [317].

The following MACS compilation of Bao *et al.* [132] was already comprising a network of 364 (n, γ) reactions, including also relevant partial cross sections, and provided detailed information on previous MACS results, which were eventually condensed into recommended values for thermal energies from 5 to 100 keV. Where experimental information was missing, calculations with the Hauser-Feshbach statistical model code NON-SMOKER [275] were empirically corrected for known systematic deficiencies in the nuclear input of the calculation. Stellar enhancement factors (SEF) were included as well.

For easy access, this compilation was published in electronic form via the KADONIS project (<http://www.kadonis.org>) [318]. The present update (KADONIS v0.3 [79]), includes 38 improved and 14 new cross sections compared to [132], in total, data for 356 isotopes, including 77 radioactive nuclei on or close to the s -process path. This version counted experimental data for 13 of these radioactive nuclei, i.e. for ^{14}C , ^{60}Fe , ^{93}Zr , ^{99}Tc , ^{107}Pd , ^{129}I , ^{135}Cs , ^{147}Pm , ^{151}Sm , ^{154}Eu , ^{163}Ho , ^{182}Hf , and ^{185}W , while empirically corrected Hauser-Feshbach rates with typical uncertainties of 25 to 30% were quoted otherwise. Presently, a new update is in preparation and should be available in 2014.

The present version of KADONIS consists of two parts: the s -process library and a collection of available experimental p -process reactions. The s -process library will be complemented in the near future by (n, p) and (n, α) cross sections measured at $k_B T = 30$ keV, as it was already included in [314]. The p -process database will be a collection of all available charged-particle reactions measured within or close to the Gamow window of the p process ($T_9 = 2\text{-}3$ GK).

6.2. Further requirements

The recommended uncertainties of the (n, γ) cross sections for s -process nucleosynthesis calculations is summarized in Figure 13 as a function of mass number (top) together with the improvements of the last decade represented by the ratio of the uncertainties (bottom). Though the necessary accuracy for stable isotopes of 1 to 5% has been locally achieved, further improvements are clearly required, predominantly below $A = 120$ and in the mass region above 180. It is worthwhile noting that some uncertainties actually increased. Those are cases, where theoretical estimates revealed larger uncertainties than before. No experimental data are available for those isotopes.

Further efforts in this field are the more important as Figure 13 reflects only the situation for a thermal energy of 30 keV. In most cases, however, the experimental data had to be extrapolated to determine the MACS values at lower and higher temperatures. Accordingly, this implies significantly larger uncertainties.

The lack of accurate data is particularly crucial for the weak s -process in massive stars, which is responsible for most of the s abundances between Cu and Sr. Since the neutron exposure of the weak s process is not sufficient for achieving flow equilibrium, cross section uncertainties may affect the abundances of a sequence of heavier isotopes

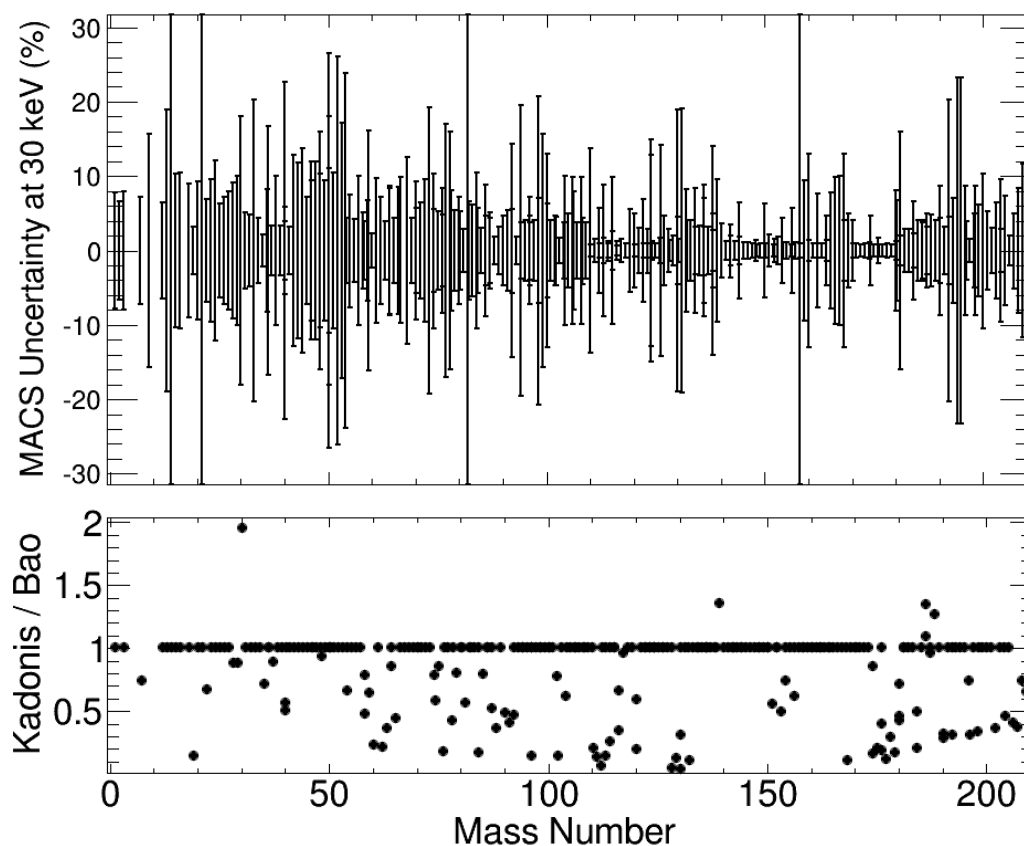


Figure 13. Top: MACS uncertainties versus mass number. Bottom: Current recommended uncertainties relative to the uncertainties in 2000 (Ref. [132]).

(see Figure 6).

A further extension of KADONIS is planned to include more radioactive isotopes, which are relevant for s -process nucleosynthesis at higher neutron densities (up to 10^{11} cm^{-3}) [319]. Because these isotopes are more than one atomic mass unit away from the canonical s -process path on the neutron-rich side of the stability valley, their stellar (n, γ) values have to be extrapolated from known cross sections by means of the statistical Hauser-Feshbach model. According to the KADONIS homepage already 73 additional unstable isotopes have been identified. The desired accuracy for radioactive branch-point isotopes is 10 to 20%.

From the above, it is obvious that experimental work should focus on two aspects, (i) on a large set of stable isotopes, where data are incomplete or too uncertain, and (ii) on the largely unexplored field of radioactive isotopes, be it the branch points in the s path or the neutron-rich nuclei at the border of stability that are reached under extreme s -process conditions at neutron densities of 10^{12} to 10^{15} cm^{-3} .

7. Summary

Neutron reactions are of pivotal importance for our understanding of how the heavy element abundances are formed during the late stellar phases. Maxwellian averaged cross sections are particularly important to constrain *s*-process models related to the H/He shell burning in AGB stars and also for the He and C shell burning phases in massive stars. The fact that the respective *s*-process abundance distributions can be deduced in quantitative detail is crucial for defining the abundances produced by explosive nucleosynthesis and for deriving a reliable picture of Galactic chemical evolution.

Continued improvements of laboratory neutron sources and of measurement techniques were instrumental for establishing a comprehensive collection of neutron-induced reaction rates in the astrophysically relevant energy range from a few up to about 300 keV. Apart from very few exceptions, experimental data are available for all stable isotopes between Fe and Pb, although not always with sufficient accuracy and in the entire energy range of interest. Such deficits are particularly found for the very small cross sections of the abundant light elements, which represent potential neutron poisons, and for neutron magic nuclei, which are the bottle necks in the *s*-process reaction flow. For the unstable species, which are needed under special *s*-process conditions characterized by high neutron densities and for explosive nucleosynthesis, experimental data are still very scarce and must so far be complemented by theory. The main role of theory, however, refers to corrections concerning the stellar environment, i.e. with respect to the effect of thermally populated excited states to the enhancement of weak interaction rates in the stellar plasma.

The main challenges for the future will be related to the further improvement of the laboratory neutron sources and to the development of advanced experimental methods. Progress in these fields is mandatory for tackling the yet unsatisfactory situation with neutron reactions of unstable isotopes. It appears that promising developments in both areas are presently under way with the potential for innovative solutions. As a consequence, future experiments can be performed with much higher sensitivities, i.e. by using very small amounts of sample material. This is crucial for dealing with unstable isotopes, because the sample activity can be reduced and the stringent problem of sample preparation can be solved by using the intense radioactive beam facilities. Within the next decade, these options will provide ample opportunities to extend neutron reaction studies into the region of unstable isotopes.

Acknowledgements

The authors would like to thank C. Guerrero, F. Gunsing, V. Vlachoudis, as well as J. Heyse and P. Schillebeeckx for providing neutron fluxes and further information about n_TOF and GELINA. Thanks are also due to R. Gallino and S. Bisterzo for their permission to use Figure 5. This work was supported by the Helmholtz Young Investigator project VH-NG-327 and the BMBF project 05P12RFFN6 and the Helmholtz International Center for FAIR.

References

- [1] Bethe H and Critchfield C 1938 *Phys. Rev.* **54** 248
- [2] von Weizsäcker C 1938 *Physik. Zeitschrift* **39** 639
- [3] Bethe H 1939 *Phys. Rev.* **55** 103
- [4] Merrill S 1952 *Ap. J.* **116** 21
- [5] Suess H and Urey H 1956 *Rev. Mod. Phys.* **28** 53–74
- [6] Cameron A 1959 *Ap. J.* **129** 676
- [7] Burbidge E, Burbidge G, Fowler W and Hoyle F 1957 *Rev. Mod. Phys.* **29** 547
- [8] Cameron A 1957 Stellar evolution, nuclear astrophysics, and nucleogenesis, chalk river report crl-41 Tech. rep. A.E.C.L. Chalk River, Canada
- [9] Cameron A 1957 *Pub. Astron. Soc. Pacific* **9** 201
- [10] Macklin R and Gibbons J 1965 *Rev. Mod. Phys.* **37** 166
- [11] Allen B, Gibbons J and Macklin R 1971 *Adv. Nucl. Phys.* **4** 205
- [12] Clayton D, Fowler W, Hull T and Zimmerman B 1961 *Ann. Phys.* **12** 331
- [13] Seeger P, Fowler W and Clayton D 1965 *Ap. J. Suppl.* **11** 121
- [14] Clayton D and Ward R 1974 *Ap. J.* **193** 397
- [15] Käppeler F, Gallino R, Busso M, Picchio G and Raiteri C 1990 *Ap. J.* **354** 630 – 643
- [16] Wisshak K, Voss F, Käppeler F, Kazakov L and Reffo G 1998 *Phys. Rev. C* **57** 391 – 408
- [17] Arlandini C, Käppeler F, Wisshak K, Gallino R, Lugaro M, Busso M and Straniero O 1999 *Ap. J.* **525** 886–900
- [18] Weigert A 1966 *Z. Astrophys.* **64** 395
- [19] Schwarzschild M and Härm R 1967 *Ap. J.* **150** 961
- [20] Sanders R 1967 *Ap. J.* **150** 971
- [21] Ulrich R 1973 *Explosive Nucleosynthesis* ed Schramm D and Arnett W (Austin: University of Texas) p 139
- [22] Truran J, Arnett W, Tsuruta S and Cameron A W 1968 *Astrophys. Space Sci.* **1** 129
- [23] Hillebrandt W 1978 *Space Sci. Rev.* **21** 639
- [24] Woosley S and Howard W 1978 *Ap. J. Suppl.* **36** 285
- [25] Rayet M, Prantzos N and Arnould M 1990 *Astron. Astrophys.* **227** 271
- [26] Goldschmidt V 1937 *Norske Vidensk. Akad. Skr. Mat.–Naturv. Kl. IV* 1
- [27] Cameron A 1982 *Essays in Nuclear Astrophysics* ed Barnes C, Schramm D and Clayton D (Cambridge: Cambridge Univ. Press) pp 23–43
- [28] Anders E and Ebihara M 1982 *Geochim. Cosmochim. Acta* **46** 2363
- [29] Anders E and Grevesse N 1989 *Geochim. Cosmochim. Acta* **53** 197
- [30] Lodders K 2003 *Ap. J.* **591** 1220
- [31] Grevesse N, Asplund M and Sauval A 2007 *Space Sci. Rev.* **130** 105–114
- [32] Lodders K, Palme H and Gail H P 2009 *Landolt–Börnstein, New Series, Vol. VI/4B, Chap. 4.4* ed Trümper J (Berlin: Springer) pp 560–630 arXiv:0901.1149 [astro-ph.EP]
- [33] Reeves H 1994 *Rev. Mod. Phys.* **66** 193
- [34] Busso M, Gallino R and Wasserburg G 1999 *Ann. Rev. Astron. Astrophys.* **37** 239
- [35] Iben I J and Renzini A 1983 *Ann. Rev. Astron. Astrophys.* **21** 271
- [36] Herwig F 2004 *Ap. J. Suppl.* **155** 651
- [37] Straniero O, Gallino R and Cristallo S 2006 *Nucl. Phys. A* **777** 311
- [38] Sneden C, Cowan J and Gallino R 2008 *Ann. Rev. Astron. Astrophys.* **46** 241
- [39] Straniero O, Chieffi A, Limongi M, Busso M, Gallino R and Arlandini C 1997 *Ap. J.* **478** 332
- [40] Gallino R, Arlandini C, Busso M, Lugaro M, Travaglio C, Straniero O, Chieffi A and Limongi M 1998 *Ap. J.* **497** 388–403
- [41] Langer N, Heger A, Wellstein S and Herwig F 1999 *Astron. Astrophys.* **346** L37
- [42] Denissenkov P and Tout C 2003 *Mon. Not. Royal Astron. Soc.* **340** 722
- [43] Herwig F, Blöcker T, Schönberner D and El Eid M 1997 *Astron. Astrophys.* **324** L81 – L84

- [44] Freytag B, Ludwig H and Steffen M 1996 *Astron. Astrophys.* **313** 497
- [45] Herwig F 2000 *Astron. Astrophys.* **360** 952
- [46] Straniero O, Cristallo S and Gallino R 2009 *Publ. Astron. Soc. Australia* **26** 133
- [47] Zinner E 1998 *Ann. Rev. Earth Planet. Sci.* **26** 147–188
- [48] Bisterzo S, Gallino R, Straniero O, Cristallo S, Käppeler F and Aoki W 2010 *Mon. Not. Royal Astron. Soc.* **404** 1529
- [49] Travaglio C, Gallino R, Busso M and Gratton R 2001 *Ap. J.* **549** 346–352
- [50] Travaglio C, Gallino R, Arnone E, Cowan J, Jordan F and Sneden C 2004 *Ap. J.* **601** 864
- [51] Serminato A, Gallino R, Travaglio C, Bisterzo S and Straniero O 2009 *Publ. Astron. Soc. Australia* **26** 153
- [52] Käppeler F, Gallino R, Bisterzo S and Aoki W 2011 *Rev. Mod. Phys.* **83** 157
- [53] Lugaro M, Herwig F, Lattanzio J, Gallino R and Straniero O 2003 *Ap. J.* **586** 1305
- [54] Couch R, Schmiedekamp A and Arnett W 1974 *Ap. J.* **190** 95
- [55] Lamb S, Howard W, Truran J and Iben I 1977 *Ap. J.* **217** 213
- [56] Arnett W and Thielemann F K 1985 *Ap. J.* **295** 589
- [57] Busso M and Gallino R 1985 *Astron. Astrophys.* **151** 205
- [58] Prantzos N, Arnould M and Arcoragi J 1987 *Ap. J.* **315** 209
- [59] Arnett W and Truran J 1969 *Ap. J.* **157** 339
- [60] Raiteri C, Busso M, Gallino R, Picchio G and Pulone L 1991 *Ap. J.* **367** 228–238
- [61] Raiteri C, Busso M, Gallino R and Picchio G 1991 *Ap. J.* **371** 665–672
- [62] Raiteri C, Gallino R and Busso M 1992 *Ap. J.* **387** 263–275
- [63] Raiteri C, Gallino R, Busso M, Neuberger D and Käppeler F 1993 *Ap. J.* **419** 207–223
- [64] Woosley S and Weaver T 1995 *Ap. J. Suppl.* **101** 181 – 235
- [65] Limongi M, Straniero O and Chieffi A 2000 *Ap. J. Suppl.* **129** 625
- [66] Woosley S, Heger A and Weaver T 2002 *Rev. Mod. Phys.* **74** 1015
- [67] The L, El Eid M and Meyer B 2007 *Ap. J.* **655** 1058
- [68] El Eid M, The L S and Meyer B 2009 *Space Sci. Rev.* **147** 1
- [69] Pignatari M, Gallino R, Heil M, Wiescher M, Käppeler F, Herwig F and Bisterzo S 2010 *Ap. J.* **710** 1557
- [70] Rauscher T and Guber K 2002 *Phys. Rev. C* **66** 028802
- [71] Rauscher T, Heger A, Hoffman R and Woosley S 2002 *Ap. J.* **576** 323
- [72] Rauscher T and Guber K 2005 *Phys. Rev. C* **71** 059903
- [73] Nassar H, Paul M, Ahmad I, Berkovits D, Bettan M, Collon P, Dababneh S, Ghelberg S, Greene J, Heger A, Heil M, Henderson D, Jiang C, Käppeler F, Koivisto H, O'Brien S, Pardo R, Patronis N, Pennington T, Plag R, Rehm K, Reifarth R, Scott R, Sinha S, Tang X and Vondrasek R 2005 *Phys. Rev. Lett.* **94** 092504
- [74] Tomyo A, Temma Y, Segawa M, Nagai Y, Makii H, Ohsaki T and Igashira M 2005 *Ap. J.* **623** L153
- [75] Alpizar-Vicente A, Bredeweg T, Esch E I, Greife U, Haight R, Hatarik R, O'Donnell J, Reifarth R, Rundberg R, Ullmann J, Vieira D and Wouters J 2008 *Phys. Rev. C* **77** 015806
- [76] Lederer C, Massimi C, Berthoumieux E, Colonna N, Dressler R, Guerrero C, Günsing F, Käppeler F, Kivel N, Pignatari M, Reifarth R, Schumann D, Wallner A, Altstadt S, Andriamonje S, Andrzejewski J, Audouin L, Barbagallo M, Bécaries V, Bečvář F, Belloni F, Berthier B, Billowes J, Boccone V, Bosnar D, Brugger M, Calviani M, Calviño F, Cano-Ott D, Carrapiço C, Cerutti F, Chiaveri E, Chin M, Cortés G, Cortés-Giraldo M A, Dillmann I, Domingo-Pardo C, Duran I, Dzysiuk N, Eleftheriadis C, Fernández-Ordóñez M, Ferrari A, Fraval K, Ganesan S, García A R, Giubrone G, Gómez-Hornillos M B, Gonçalves I F, González-Romero E, Gramegna F, Griesmayer E, Gurusamy P, Harrisopulos S, Heil M, Ioannides K, Jenkins D G, Jericha E, Kadi Y, Karadimos D, Korschinek G, Krťicka M, Kroll J, Langer C, Lebbos E, Leeb H, Leong L S, Losito R, Lozano M, Manousos A, Marganiec J, Marrone S, Martinez T, Mastinu P F, Mastromarco M, Meaze M, Mendoza E, Mengoni A, Milazzo P M, Mingrone F, Mirea M,

- Mondalaers W, Paradela C, Pavlik A, Perkowski J, Plag R, Plompen A, Praena J, Quesada J M, Rauscher T, Riego A, Roman F, Rubbia C, Sarmiento R, Schillebeeckx P, Schmidt S, Tagliente G, Tain J L, Tarrío D, Tassan-Got L, Tsinganis A, Tlustos L, Valenta S, Vannini G, Variale V, Vaz P, Ventura A, Vermeulen M J, Versaci R, Vlachoudis V, Vlastou R, Ware T, Weigand M, Weiß C, Wright T J, Žugec P and n TOF Collaboration 2014 *Phys. Rev. C* **89** 025810
- [77] Heil M, Käppeler F, Uberseder E, Gallino R and Pignatari M 2008 *Phys. Rev. C* **77** 015808
- [78] Heil M, Käppeler F, Uberseder E, Gallino R, Bisterzo S and Pignatari M 2008 *Phys. Rev. C* **78** 025802
- [79] Dillmann I, Plag R, Käppeler F and Rauscher T 2009 *EFNUDAT Fast Neutrons - scientific workshop on neutron measurements, theory & applications* ed Hamsch F J (Geel: JRC-IRMM) pp 55 – 58 <http://www.kadonis.org>
- [80] Bennett M, Hirschi R, Pignatari M, Diehl S, Fryer C, Herwig F, Hungerford A, Nomoto K, Rockefeller G, Timmes F and Wiescher M 2012 *Mon. Not. Royal Astron. Soc.* **420** 3047–3070
- [81] Westin J, Sneden C, Gustafsson B and Cowan J 2000 *Ap. J.* **530** 783
- [82] Burris D, Pilachowski C, Armandroff T, Sneden C, Cowan J and Roe H 2000 *Ap. J.* **544** 302
- [83] Cowan J, Sneden C, Burles S, Ivans I, Beers T, Truran J, Lawler J, Primas F, Fuller G, Pfeiffer B and Kratz K L 2002 *Ap. J.* **572** 861
- [84] Hill V, Plez B, Cayrel R, Beers T C, Nordström B, Andersen J, Spite M, Spite F, Barbuy B, Bonifacio P, Depagne E, François P and Primas F 2002 *Astron. Astrophys.* **387** 560
- [85] Cowan J, Sneden C, Beers T C, Lawler J E, Simmerer J, Truran J W, Primas F, Collier J and Burles S 2005 *Ap. J.* **627** 238
- [86] Cowan J and Sneden C 2006 *Nature* **440** 1151–1156
- [87] Thielemann F K, Arcones A, Kppeli R, Liebendörfer M, Rauscher T, Winteler C, Fröhlich C, Dillmann I, Fischer T, Martinez-Pinedo G, Langanke K, Farouqi K, Kratz K L, Panov I and Korneev I 2011 *Progress in Particle and Nuclear Physics* **66** 346–353
- [88] Kratz K L, Gabelmann H, Hillebrandt W, Pfeiffer B, Schlösser K and Thielemann F K 1986 *Z. Physik* **325** 489–490
- [89] Kratz K L 1988 *Rev. Mod. Astron.* **1** 184
- [90] Kratz K L, Bitouzet J P, Thielemann F K, Möller P and Pfeiffer B 1993 *Ap. J.* **403** 216–238
- [91] Wanajo S 2007 *Ap. J.* **666** L77
- [92] Woosley S and Hoffman R 1992 *Ap. J.* **395** 202
- [93] Cowan J and Thielemann F K 2004 *Physics Today* **57** 45
- [94] Kratz K L, Farouqi K and Pfeiffer B 2007 *Prog. Particle Nucl. Phys.* **59** 147–155
- [95] Nakamura K, Kajino T, Mathews G, Sato S and Harikae S 2013 *Int. J. Mod. Phys. E* **22** 1330022
- [96] Freiburghaus C, Rosswog S and Thielemann F K 1999 *Ap. J.* **525** L121
- [97] Kratz K L, Harms V, Hillebrandt W, Pfeiffer B, Thielemann F K and Wöhr A 1990 *Z. Phys. A.* **336** 357
- [98] Möller P and Nix R 1988 *Atomic Data Nucl. Data Tables* **39** 213
- [99] Rauscher T 2005 *Nucl. Phys. A* **758** 655c
- [100] Surman R and Engel J 2001 *Phys. Rev. C* **64** 035801
- [101] Arcones A and Martinez-Pinedo G 2011 *Phys. Rev. C* **83** 045809
- [102] Surman R, Engel J, Bennett J and Meyer B 1997 *Phys. Rev. Lett.* **79** 1809 – 1812
- [103] Mumpower M, McLaughlin G and Surman R 2012 *Phys. Rev. C* **85** 045801
- [104] Surman R, Beun J, McLaughlin G and Hix W 2009 *Phys. Rev. C* **79** 045809
- [105] Beun J, Blackmon J, Hix W, McLaughlin G, Smith M and Surman R 2009 *J. Phys. G* **36** 025201
- [106] Goriely S 1997 *Astron. Astrophys.* **325** 414–424
- [107] Mathews G, Mengoni A, Thielemann F K and Fowler W 1983 *Ap. J.* **270** 740
- [108] Kozub R, Arbanas G, Adekola A, Bardayan D, Blackmon J, Chae K, Chipps K, Cizewski J, Erikson L, Hatarik R, Hix W, Jones K, Krolas W, Liang J, Ma Z, Matei C, Moazen B, Nesaraja C, Pain S, Shapira D, Shriner J, Smith M and Swan T 2012 *Phys. Rev. Lett.* **109** 172501

- [109] Panov I and Thielemann F 2004 *Astron. Lett.* **30** 647
- [110] Panov I, Korneev I, Rauscher T and Thielemann F 2011 *Bull. Russ. Acad. Sci. Phys.* **75** 484
- [111] Rayet M, Arnould M, Hashimoto M, Prantzos N and Nomoto K 1995 *Astron. Astrophys.* **298** 517 – 527
- [112] Fröhlich C, Martínez-Pinedo G, Liebendörfer M, Thielemann F K, Bravo E, Hix W, Langanke K and Zinner N 2006 *Phys. Rev. Lett.* **96** 142502
- [113] Schatz H, Aprahamian A, Görres J, Wiescher M, Rauscher T, Rembges J, Thielemann F K, Pfeiffer B, Möller P, Kratz K L, Herndl H, Brown B and Rebel H 1998 *Physics Reports* **294** 167
- [114] Schatz H, Aprahamian A, V B, Bildsten L, Cumming A, Ouellette M, Rauscher T, Thielemann F K and Wiescher M 2001 *Phys. Rev. Letters* **86** 3471 – 3474
- [115] Woosley S, Hartmann D, Hoffman R and Haxton W 1990 *Ap. J.* **356** 272
- [116] Travaglio C, Röpke F, Gallino R and Hillebrandt W 2011 *Ap. J.* **739** 93
- [117] Rapp W, Görres J, Wiescher M, Schatz H and Käppeler F 2006 *Ap. J.* **653** 474
- [118] Arnould M and Goriely S 2003 *Phys. Rep.* **384** 1
- [119] Rauscher T, Dauphas N, Dillmann I, Fröhlich C, Fülöp Z and Gyürky G 2013 *Rep. Prog. Phys.* **76** 066201
- [120] Travaglio C, Galli D, Gallino R, Busso M, Ferrini F and Straniero O 1999 *Ap. J.* **521** 691
- [121] Travaglio C, Galli D and Burkert A 2001 *Ap. J.* **547** 217
- [122] Qian Y Z and Wasserburg G 2007 *Phys. Rep.* **442** 237
- [123] Farouqi K, Kratz K L, Pfeiffer B, Rauscher T, Thielemann F K and Truran J 2010 *Ap. J.* **712** 1359–1377
- [124] Maiorca E, Magrini L, Busso M, Randich S, Palmerini S and Trippella O 2012 *Astrophys. J.* **747** 53
- [125] Montes F, Beers T, Cowan J, Elliot T, Farouqi K, Gallino R, Heil M, Kratz K L, Pfeiffer B, Pignatari M and Schatz H 2007 *Ap. J.* **671** 1685
- [126] Honda S, Aoki W, Ishimaru Y, Wanajo S and Ryan S 2006 *Ap. J.* **643** 1180
- [127] Sneden C, Cowan J, Lawler J, Ivans I, Burles S, Beers T, Primas F, Hill V, Truran J, Fuller G, Pfeiffer B and Kratz K L 2003 *Ap. J.* **591** 936–953
- [128] Herwig F, Pignatari M, Woodward P R, Porter D H, Rockefeller G, Fryer C L, Bennett M and Hirschi R 2011 *Ap. J.* **727** 89 (*Preprint* 1002.2241)
- [129] García-Hernández D A, Zamora O, Yagüe A, Uttenthaler S, Karakas A I, Lugaro M, Ventura P and Lambert D L 2013 *Astron. Astrophys.* **555** L3 (*Preprint* 1306.2134)
- [130] Hinkelmann M and for the FAIR Joint Core Team 2010 Facility for antiproton and ion research Tech. rep. FAIR Newsletter No. 15 <https://www-alt.gsi.de/documents/DOC-2010-Apr-60-1.pdf>
- [131] Käppeler F, Beer H and Wisshak K 1989 *Rep. Prog. Phys.* **52** 945–1013
- [132] Bao Z, Beer H, Käppeler F, Voss F, Wisshak K and Rauscher T 2000 *Atomic Data Nucl. Data Tables* **76** 70–154
- [133] Szücs T, Dillmann I, Plag R and Fülöp Z 2010 *NIC-XI* ed Blaum K, Christlieb N and Martínez-Pinedo G (Trieste: Proceedings of Science) p 247
- [134] Moxon M and Rae E 1963 *Nucl. Instr. Meth.* **24** 445
- [135] Wisshak K and Käppeler F 1978 *Nucl. Sci. Eng.* **66** 363 – 377
- [136] Wisshak K and Käppeler F 1979 *Nucl. Sci. Eng.* **69** 39 – 46
- [137] Rau F 1963 *Nukleonik* **5** 191 – 197
- [138] Macklin R and Gibbons J 1967 *Phys. Rev.* **159** 1007–1012 based on H. Maier-Leibnitz, priv. comm. and Rau, F., *Nukleonik*, 5 (1963) 191
- [139] Koehler P, Winters R, Guber K, Rauscher T, Harvey J, Raman S, Spencer R, Blackmon J, Larson D, Bardayan D and Lewis T 2000 *Phys. Rev. C* **62** 055803
- [140] Guber K, Leal L, Sayer R, Koehler P, Valentine T, Derrien H and Harvey J 2005 *Nucl. Instr. Meth. B* **241** 218–222
- [141] Guber K, Leal L, Sayer R, Koehler P, Valentine T, Derrien H and Harvey J 2005 *Nuclear Data*

- for *Science and Technology* ed Haight R, Chadwick M, Kawano T and Talou P (New York: AIP) pp 1706–1711 aIP Conference Series 769
- [142] Plag R, Heil M, Käppeler F, Pavlopoulos P, Reifarh R and Wisshak K 2003 *Nucl. Instr. Meth. A* **496** 425 – 436
- [143] Wisshak K, Guber K, Käppeler F, Krisch J, Müller H, Rupp G and Voss F 1990 *Nucl. Instr. Meth. A* **292** 595 – 618
- [144] Guerrero C, Abbondanno U, Aerts G, Álvarez H, Álvarez-Velarde F, Andriamonje S, Andrzejewski J, Assimakopoulos P, Audouin L, Badurek G, Baumann P, Bečvář F, Berthoumieux E, Calviño F, Calviani M, Cano-Ott D, Capote R, Carrapiço C, Cennini P, Chepel V, Chiaveri E, Colonna N, Cortes G, Couture A, Cox J, Dahlfors M, David S, Dillmann I, Domingo-Pardo C, Dridi W, Duran I, Eleftheriadis C, Ferrant L, Ferrari A, Ferreira-Marques R, Fujii K, Furman W, Goncalves I, González-Romero E, Gramegna F, Günsing F, Haas B, Haight R, Heil M, Herrera-Martinez A, Igashira M, Jericha E, Käppeler F, Kadi Y, Karadimos D, Kerveno M, Koehler P, Kossionides E, Krčićka M, Lampoudis C, Leeb H, Lindote A, Lopes I, Lozano M, Lukic S, Marganec J, Marrone S, Martínez T, Massimi C, Mastinu P, Mendoza E, Mengoni A, Milazzo P M, Moreau C, Mosconi M, Neves F, Oberhummer H, O'Brien S, Pancin J, Papachristodoulou C, Papadopoulos C, Paradela C, Patronis N, Pavlik A, Pavlopoulos P, Perrot L, Pigni M T, Plag R, Plompen A, Plukis A, Poch A, Praena J, Pretel C, Quesada J, Rauscher T, Reifarh R, Rubbia C, Rudolf G, Rullhusen P, Salgado J, Santos C, Sarchiapone L, Savvidis I, Stephan C, Tagliente G, Tain J L, Tassan-Got L, Tavora L, Terlizzi R, Vannini G, Vaz P, Ventura A, Villamarin D, Vicente M C, Vlachoudis V, Vlastou R, Voss F, Walter S, Wiescher M and Wisshak K 2009 *Nucl. Instr. Meth. A* **608** 424
- [145] Heil M, Reifarh R, Fowler M, Haight R, Käppeler F, Rundberg R, Seabury E, Ullmann J, Wilhelmy J, Wisshak K and Voss F 2001 *Nucl. Instr. Meth. A* **459** 229 – 246
- [146] Reifarh R, Bredeweg T A, Alpizar-Vicente A, Browne J C, Esch E I, Greife U, Haight R C, Hatarik R, Kronenberg A, O'Donnell J M, Rundberg R S, Ullmann J L, Vieira D J, Wilhelmy J B and Wouters J M 2004 *Nucl. Instr. Meth. A* **531** 530–543
- [147] Muradyan G, Adamchuk A, Adamchuk V, Shchepkin Y and Voskanyan M 1985 *Nucl. Sci. Eng.* **90** 60
- [148] Block R, Danon Y, Slovacek R, Werner C and Youk G 1994 *Nuclear Data for Science and Technology* ed Dickens J (La Grange Park, Illinois: American Nuclear Society) p 81
- [149] Brehm K, Becker H, Rolfs C, Trautvetter H, Käppeler F and Ratynski W 1988 *Z. Phys. A* **330** 167 – 172
- [150] Koehler P and O'Brien H 1989 *Phys. Rev. C* **39** 1655
- [151] Schatz H, Jaag S, Linker G, Steininger R, Käppeler F, Koehler P, Graff S and Wiescher M 1995 *Phys. Rev. C* **51** 379 – 391
- [152] Wagemans C, Weigmann H and Barthelemy R 1987 *Nucl. Phys. A* **469** 497
- [153] De Smet L, Wagemans C, Wagemans J, Heyse J and Van Gils J 2007 *Phys. Rev. C* **76** 045804
- [154] Gledenov Y, Koehler P, Andrzejewski K, Guber K and Rauscher T 2000 *Phys. Rev. C* **62** 42801
- [155] Andriamonje S, Attie D, Berthoumieux E, Calviani M, Colas P, Dafni T, Fanourakis G, Ferrer-Ribas E, Galan J, Gerasis T, Giganon A, Giomataris I, Gris A, Guerrero Sanchez C, Günsing F, Iguaz F, Irastorza I, De Oliveira R, Papaevangelou T, Ruz J, Savvidis I, A T and Toms A 2010 *J. Instrumentation* **5** P02001
- [156] Giomataris Y, Rebourgeard P, Robert J and Charpark G 1996 *Nucl. Instr. Meth. Phys. Res. A* **376** 29
- [157] Andriamonje S, Calviani M, Kadi Y, Losito R, Vlachoudis V, Berthoumieux E, Günsing F, Giomataris Y, Papaevangelou T, Guerrero C, Colonna N, Weiss C and the n_TOF Collaboration 2011 *J. Korean Phys. Soc.* **59** 1601
- [158] Calviani M, Cennini P, Karadimos D, Ketlerov V, Konovalov V, Furman W, Goverdowski A, Vlachoudis V, Zanini L and the n_TOF Collaboration 2008 *Nucl. Instr. Meth. A* **594** 220 227
- [159] Tassan-Got L, Berthier B, Duran I, Ferrant L, Isaev S, de la Naour C, Paradela C, Stephan

- C, Trubert D and the n_TOF Collaboration 2005 *International Conference on Nuclear Data for Science and Technology* ed Haight R, Chadwick M, Kawano T and Talou P (New York: American Institute of Physics) p 1529 AIP Conference Series 769
- [160] Tarrío D, Leong L S, Audouin L, Duran I, Paradela C, Tassan-Got L, Le Naour C, Bacri C O, Petitbon V, Mottier J, Caamaño M, Altstadt S, Andrzejewski J, Barbagallo M, Bécares V, Bečvář F, Belloni F, Berthoumieux E, Billowes J, Boccone V, Bosnar D, Brugger M, Calviani M, Calviño F, Cano-Ott D, Carrapiço C, Cerutti F, Chiaveri E, Chin M, Colonna N, Cortés G, Cortés-Giraldo M A, Diakaki M, Domingo-Pardo C, Dzysiuk N, Eleftheriadis C, Ferrari A, Fraval K, Ganesan S, García A R, Giubrone G, Gómez-Hornillos M B, Gonçalves I F, González-Romero E, Griesmayer E, Guerrero C, Günsing F, Gurusamy P, Jenkins D G, Jericha E, Kadi Y, Käppeler F, Karadimos D, Koehler P, Kokkoris M, Krtička M, Kroll J, Langer C, Lederer C, Leeb H, Losito R, Manousos A, Marganec J, Martínez T, Massimi C, Mastinu P F, Mastromarco M, Meaze M, Mendoza E, Mengoni A, Milazzo P M, Mingrone F, Mirea M, Mondalaers W, Pavlik A, Perkowski J, Plompen A, Praena J, Quesada J M, Rauscher T, Reifarh R, Riego A, Roman F, Rubbia C, Sarmiento R, Schillebeeckx P, Schmidt S, Tagliente G, Tain J L, Tsinganis A, Valenta S, Vannini G, Variale V, Vaz P, Ventura A, Versaci R, Vermeulen M J, Vlachoudis V, Vlastou R, Wallner A, Ware T, Weigand M, Weiß C, Wright T J and Žugec P 2014 *Nuclear Instruments and Methods in Physics Research A* **743** 79–85
- [161] Koehler P and Graff S 1991 *Phys. Rev. C* **44** 2788
- [162] Marrone S, Mastinu P F, Abbondanno U, Bacconi R, Marchi E B, Bustreo N, Colonna N, Gramegna F, Loriggiola M, Marigo S, Milazzo P M, Moreau C, Sacchetti M, Tagliente G, Terlizzi R, Vannini G, Aerts G, Berthoumieux E, Cano-Ott D, Cennini P, Domingo-Pardo C, Ferrant L, Gonzalez-Romero E, Günsing F, Heil M, Kaeppler F, Papaevangelou T, Paradela C, Pavlopoulos P, Perrot L, Plag R, Tain J L, Wendler H and n TOF Collaboration 2004 *Nucl. Instr. Meth. Phys. Res. A* **517** 389 – 398
- [163] Weiß C, Griesmayer E, Guerrero C, Altstadt S, Andrzejewski J, Audouin L, Badurek G, Barbagallo M, Bécares V, Bečvář F, Belloni F, Berthoumieux E, Billowes J, Boccone V, Bosnar D, Brugger M, Calviani M, Calviño F, Cano-Ott D, Carrapiço C, Cerutti F, Chiaveri E, Chin M, Colonna N, Cortés G, Cortés-Giraldo M, Diakaki M, Domingo-Pardo C, Duran I, Dressler R, Dzysiuk N, Eleftheriadis C, Ferrari A, Fraval K, Ganesan S, Garca A, Giubrone G, Gómez-Hornillos M, Gonalves I, González-Romero E, Günsing F, Gurusamy P, Hernández-Prieto A, Jenkins D, Jericha E, Kadi Y, Käppeler F, Karadimos D, Kivel N, Koehler P, Kokkoris M, Krtička M, Kroll J, Lampoudis C, Langer C, Leal-Cidoncha E, Lederer C, Leeb H, Leong L, Losito R, Mallick A, Manousos A, Marganec J, Martinez T, Massimi C, Mastinu P, Mastromarco M, Meaze M, Mendoza E, Mengoni A, Milazzo P, Mingrone F, Mirea M, Mondalaers W, Paradela C, Pavlik A, Perkowski J, Plompen A, Praena J, Quesada J, Rauscher T, Reifarh R, Riego A, Robles M, Roman F, Rubbia C, Sabaté-Gilarte M, Sarmiento R, Saxena A, Schillebeeckx P, Schmidt S, Schumann D, Tagliente G, Tain J, Tarrío D, Tassan-Got L, Tsinganis A, Valenta S, Vannini G, Variale V, Vaz P, Ventura A, Versaci R, Vermeulen M, Vlachoudis V, Vlastou R, Wallner A, Ware T, Weigand M, Wright T and Žugec P 2013 *Nucl. Instr. Meth. A* **732** 190 – 194
- [164] Ratynski W and Käppeler F 1988 *Phys. Rev. C* **37** 595–604
- [165] Lederer C, Käppeler F, Mosconi M, Nolte R, Heil M, Reifarh R, Schmidt S, Dillmann I, Giesen U, Mengoni A and Wallner A 2012 *Phys. Rev. C* **85** 055809
- [166] Feinberg G, Friedman M, Krasa A, Shor A, Eisen Y, Berkovits D, Giorginis G, Hirsh T, Paul M, Plompen A and Tsuk E 2012 *Phys. Rev. C* **85** 055810
- [167] Heil M, Dababneh S, Juseviciute A, Käppeler F, Plag R, Reifarh R and O'Brien S 2005 *Phys. Rev. C* **71** 025803
- [168] Käppeler F, Naqvi A and Al-Ohali M 1987 *Phys. Rev. C* **35** 936–941
- [169] Beer H 1991 *Ap. J.* **375** 823
- [170] Reifarh R, , Heil M, Forssén C, Besserer U, Couture A, Dababneh S, Dörr L, Görres J, Haight

- R, Käppeler F, Mengoni A, O'Brien S, Patronis N, Plag R, Rundberg R, Wiescher M and Wilhelmy J 2008 *Phys. Rev. C* **77** 015804
- [171] Meissner J, Schatz H, Görres J, Herndl H, Wiescher M, Beer H and Käppeler F 1996 *Phys. Rev. C* **53** 459 – 468
- [172] Beer H, Rupp G, Walter G, Voss F and Käppeler F 1994 *Nucl. Instr. Meth. A* **337** 492 – 503
- [173] Patronis N, Dababneh S, Assimakopoulos P, Gallino R, Heil M, Käppeler F, Karamanis D, Koehler P, Mengoni A and Plag R 2004 *Phys. Rev. C* **69** 025803
- [174] Reifarh R, Arlandini C, Heil M, Käppeler F, Sedyshev P, Herman M, Rauscher T, Gallino R and Travaglio C 2003 *Ap. J.* **582** 1251 – 1262
- [175] Jaag S and Käppeler F 1995 *Phys. Rev. C* **51** 3465 – 3471
- [176] Jaag S and Käppeler F 1996 *Ap. J.* **464** 874–883
- [177] Reifarh R, Haight R, Heil M, Fowler M, Käppeler F, Miller G, Rundberg R, Ullmann J and Wilhelmy J 2003 *Nucl. Phys.* **A718** 478c
- [178] Vockenhuber C, Dillmann I, Heil M, Käppeler F, Wallner A and Winckler N 2007 *Phys. Rev. C* **75** 015804
- [179] Uberseder E, Reifarh R, Schumann D, Dillmann I, Domingo Pardo C, Görres J, Heil M, Käppeler F, Marganec J, Neuhausen J, Pignatari M, Voss F, Walter S and Wiescher M 2009 *Phys. Rev. Lett.* **102** 151101
- [180] Schumann D, Neuhausen J, Dillmann I, Domingo Pardo C, Käppeler F, Marganec J, Voss F, Walter S, Heil M, Reifarh R, Görres J, Uberseder E and Wiescher M 2010 *Nucl. Instr. Meth. A* **613** 347
- [181] Paul M, Henning W, Kutschera W, Stephenson E and Yntema J 1980 *Phys. Lett. B* **94** 303
- [182] Dillmann I, Faestermann T, Korschinek G, Lachner J, Maiti M, Poutivtsev M, Rugel G, Walter S, Käppeler F, Erhard M, Junghans A, Nair C, Schwengner R and Wagner A 2010 *Nucl. Instr. Meth. B* **268** 1283
- [183] Wallner A, Coquard L, Dillmann I, Forstner O, Golser R, Heil M, Käppeler F, Kutschera W, Mengoni A, Michlmayr L, Priller A, Steier P and Wiescher M 2008 *J. Phys. G: Nucl. Part. Phys.* **35** 014018
- [184] Wallner A, Buczak K, Dillmann I, Feige J, Käppeler F, Korschinek G, Lederer C, Mengoni A, Ott U, Paul M, Schätzel G, Steier P and Trautvetter H 2012 *Publications of the Astronomical Society of Australia* **29** 115
- [185] Dillmann I, Heil M, Käppeler F, Wallner A, Kutschera W, Priller A, Steier P and Paul M 2009 *Phys. Rev. C* **79** 065805
- [186] Coquard L, Dillmann I, Wallner A, Käppeler F and Kutschera W 2006 *Nuclei in the Cosmos-IX* <http://pos.sissa.it/> ed Mengoni A and et al (SISSA: Proceedings of Science) p contribution 274
- [187] Rugel G, Dillmann I, Faestermann T, Heil M, Käppeler F, Knie K, Korschinek G, Kutschera W, Poutivtsev M and Wallner A 2007 *Nucl. Instr. Meth. B* **259** 683
- [188] Dillmann I, Heil M, Käppeler F, Faestermann T, Korschinek G, Knie K, Poutivtsev M, Rugel G, Wallner A and Rauscher T 2006 *Nuclei in the Cosmos-IX* <http://pos.sissa.it> ed Mengoni A and et al (SISSA, Trieste: Proceedings of Science) p contribution 089
- [189] Nakamura T, Fukuda N, Aoi N, Imai N, Ishihara M, Iwasaki H, Kobayashi T, Kubo T, Mengoni A, Motobayashi T, Notani M, Otsu H, Sakurai H, Shimoura S, Teranishi T, Watanabe Y X and Yoneda K 2009 *Phys. Rev. C* **79** 035805
- [190] Datta Pramanik U, Aumann T, Boretzky K, Carlson B, Cortina D, Elze T, Emling H, Geissel H, Grünschloß A, Hellström M, Ilievski S, Kratz J, Kulessa R, Leifels Y, Leistenschneider A, Lubkiewicz E, Münzenberg G, Reiter P, Simon H, Sümmerer K, Wajda E and Walus W 2003 *Phys. Lett. B* **551** 63
- [191] Boretzky K, Agrawal B, Alkhasov G, Andreev G, Aumann T, Basu P, Bemmerer D, Bertini D, Bhattacharya P, Bhattacharya S, Blanco A, Caesar C, Chakraborty S, Chatterjee S, Cherciu M, Chulkov L, Ciobanu M, Cowan T, Datta Pramanik U, Elekes Z, Endres J, Fetisov A, Fonte P, Galaviz D, Golotsov V, Haiduc M, Hehner J, Heil M, Heinz A, Hennig A, Ignatov A, Ickert

- G, Ivanov E, Kempe M, Kresan D, Krivshich A, Kumar Das P, Leifels Y, Lopez L, Machado J, Maroussov V, Panja J, Potlog M, Rahaman A, Ray A, Reifarh R, Röder M, Rossi D, Roy J, Scheit H, Simon H, Sinha T, Sobiella M, Stach D, Stan E, Teubig P, Uvarov L, Vikhrov V, Volkmandt M, Volkov S, Wagner A, Wüstenfeld J, Yakorev D, Zhdanov A, Zilges A and Zuber K 2011 Neuland@r3b: A fully-active detector for time-of-flight and calorimetry of fast neutrons Tech. rep. GSI, Darmstadt gSI Sci. Rep., PHN-NUSTAR-NR-02, p. 174
- [192] Sonnabend K, Mohr P, Vogt K, Zilges A, Mengoni A, Rauscher T, Beer H, Käppeler F and Gallino R 2003 *Ap. J.* **583** 506 – 513
- [193] Weller H 2008 *Progress in Nuclear and Particle Physics* **62** 257 – 303
- [194] Escher J, Ahle L, Bernstein L, Church J, Dietrich F, Forssén C and Hoffman R 2005 *Nucl. Phys. A* **758** 86 – 89
- [195] Forssén C, Dietrich F S, Escher J, Hoffman R D and Kelley K 2007 *Physical Review C (Nuclear Physics)* **75** 055807
- [196] Escher J, Burke J, Dietrich F, Scielzo N, Thompson I and Younes W 2012 *Rev. Mod. Phys.* **84** 353
- [197] Abbondanno U, Andriamonje S, Andrzejewski J, Angelopoulos A, Assimakopoulos P, Bacri C O, Badurek G, Beer H, Berthier B, Bondarenko I, Bos A, Bustreo N, Calvino F, Cano-Ott D, Capote R, Carlson P, Charpak G, Chauvin N, Cennini P, Chepel V, Colonna N, Cortes G, Corvi F, Damianoglou D, David S, Dimovasili E, Domingo C, Doroshenko A, Duran Escribano I, Eleftheriadis C, Embid M, Ferrant L, Ferrari A, Ferreira-Marques R, Fraiss-Koelbl H, Furman W, Fursov B, Garzon J A, Giomataris I, Gledenov Y, Gonzalez-Romero E, Goverdovski A, Gramegna F, Griesmayer E, Günsing F, Haight R, Heil M, Hollander P, Ioannides K, Ioannu P, Isaev S, Jericha E, Kadi Y, Käppeler F, Karadimos D, Karamanis D, Kayukov A, Kazakov L, Kelic A, Ketlerov V, Kitis G, Koehler P, Kopach Y, Kossionides E, Kroshkina I, Lacoste V, Lamboudis C, Leeb H, Lepretre A, Lopes M, Lozano M, Marrone S, Martinez-Val J, Mastinu P, Mengoni A, Meunier R, Mezentseva J, Milazzo P, Minguiez E, Mitrofanov V, Nicolis N, Nikolenko V, Oberhummer H, Pakou A, Pancin J, Papadopoulos K, Papaevangelou T, Paradela C, Paradellis T, Pavlik A, Pavlopoulos P, Perez-Parra A, Perriale L, Perlendo J, Peskov V, Pikaikin V, Plag R, Plompen A, Poch A, Policarpo A, Popov A, Popov Y, Pretel C, Quesada J, Radermacher E, Rauscher T, Reifarh R, Rejmund F, Rubbia C, Rudolf G, Rullhusen P, Sakelliou L, Saldana F, Tagliente G, Tain J, Tapia C, Tassan-Got L, Terchychnyi R, Tsabaris C, Tsangas N, van Eijk C, Vannini G, Ventura A, Villamarin A, Vlachoudis V, Vlastou R, Voinov A, Voss F, Wendler H, Wiescher M, Wisshak K, Zeinalov S and Zhuravlev B 2001 Neutron tof facility (ps213) status report Tech. rep. CERN, Geneva, Switzerland report CERN/INTC 2001-021
- [198] Chiaveri E, Calviani M, Vlachoudis V, Weiss C and the n_TOF collaboration 2012 *Compound nuclear reactions and related topics* vol 21 (EPJ Web of Conferences)
- [199] Guerrero C, Tsinganis A, Berthoumieux E, Barbagallo M, Belloni F, Günsing F, Weiß C, Chiaveri E, Calviani M, Vlachoudis V, Altstadt S, Andriamonje S, Andrzejewski J, Audouin L, Bécères V, Bečvář F, Billowes J, Boccone V, Bosnar D, Brugger M, Calviño F, Cano-Ott D, Carrapiço C, Cerutti F, Chin M, Colonna N, Cortés G, Cortés-Giraldo M A, Diakaki M, Domingo-Pardo C, Duran I, Dressler R, Dzysiuk N, Eleftheriadis C, Ferrari A, Fraval K, Ganesan S, García A R, Giubrone G, Göbel K, Gómez-Hornillos M B, Gonçalves I F, González-Romero E, Griesmayer E, Gurusamy P, Hernández-Prieto A, Gurusamy P, Jenkins D G, Jericha E, Kadi Y, Käppeler F, Karadimos D, Kivel N, Koehler P, Kokkoris M, Kratička M, Kroll J, Lampoudis C, Langer C, Leal-Cidoncha E, Lederer C, Leeb H, Leong L S, Losito R, Manousos A, Marganec J, Martínez T, Massimi C, Mastinu P F, Mastro marco M, Meaze M, Mendoza E, Mengoni A, Milazzo P M, Mingrone F, Mirea M, Mondalaers W, Papaevangelou T, Paradela C, Pavlik A, Perkowski J, Plompen A, Praena J, Quesada J M, Rauscher T, Reifarh R, Riego A, Roman F, Rubbia C, Sabate-Gilarte M, Sarmiento R, Saxena A, Schillebeecx P, Schmidt S, Schumann D, Steinegger P, Tagliente G, Tain J L, Tarrío D, Tassan-Got L, Valenta S, Vannini G, Variale V, Vaz P,

- Ventura A, Versaci R, Vermeulen M J, Vlastou R, Wallner A, Ware T, Weigand M, Wright T and Žugec P 2013 *Eur. Phys. J. A* **49** 27
- [200] Lisowski P, Bowman C, Russell G and Wender S 1990 *Nucl. Sci. Eng.* **106** 208
- [201] J-PARC 2008 J-parc annual report 2008 Tech. rep. http://j-parc.jp/documents/annual_report/a_report_2008.pdf
- [202] Lederer C and the n_TOF collaboration 2013 *Nuclear Data for Science and Technology* (New York: BNL)
- [203] Tagliente G, Milazzo P M, Fujii K, Abbondanno U, Aerts G, Álvarez H, Alvarez-Velarde F, Andriamonje S, Andrzejewski J, Audouin L, Badurek G, Baumann P, Bečvář F, Belloni F, Berthoumieux E, Bisterzo S, Calviño F, Calviani M, Cano-Ott D, Capote R, Carrapiço C, Cennini P, Chepel V, Chiaveri E, Colonna N, Cortes G, Couture A, Cox J, Dahlfors M, David S, Dillmann I, Domingo-Pardo C, Dridi W, Duran I, Eleftheriadis C, Embid-Segura M, Ferrari A, Ferreira-Marques R, Furman W, Gallino R, Goncalves I, Gonzalez-Romero E, Gramegna F, Guerrero C, Günsing F, Haas B, Haight R, Heil M, Herrera-Martinez A, Jericha E, Käppeler F, Kadi Y, Karadimos D, Karamanis D, Kerveno M, Kossionides E, Kratička M, Lamboudis C, Leeb H, Lindote A, Lopes I, Lozano M, Lukic S, Marganiec J, Marrone S, Martínez T, Massimi C, Mastinu P, Mengoni A, Moreau C, Mosconi M, Neves F, Oberhummer H, O'Brien S, Pancin J, Papachristodoulou C, Papadopoulos C, Paradela C, Patronis N, Pavlik A, Pavlopoulos P, Perrot L, Pigni M T, Plag R, Plompen A, Plukis A, Poch A, Praena J, Pretel C, Quesada J, Rauscher T, Reifarh R, Rosetti M, Rubbia C, Rudolf G, Rullhusen P, Salgado J, Santos C, Sarchiapone L, Savvidis I, Stephan C, Tain J L, Tassan-Got L, Tavora L, Terlizzi R, Vannini G, Vaz P, Ventura A, Villamarin D, Vincente M C, Vlachoudis V, Vlastou R, Voss F, Walter S, Wiescher M and Wisshak K 2011 *Phys. Rev. C* **84** 015801
- [204] Tagliente G, Milazzo P M, Fujii K, Abbondanno U, Aerts G, Álvarez H, Alvarez-Velarde F, Andriamonje S, Andrzejewski J, Audouin L, Badurek G, Baumann P, Bečvář F, Belloni F, Berthoumieux E, Calviño F, Calviani M, Cano-Ott D, Capote R, Carrapiço C, Cennini P, Chepel V, Chiaveri E, Colonna N, Cortes G, Couture A, Dahlfors M, David S, Dillmann I, Domingo-Pardo C, Dridi W, Duran I, Eleftheriadis C, Embid-Segura M, Ferrari A, Ferreira-Marques R, Furman W, Goncalves I, Gonzalez-Romero E, Gramegna F, Guerrero C, Günsing F, Haas B, Haight R, Heil M, Herrera-Martinez A, Jericha E, Käppeler F, Kadi Y, Karadimos D, Karamanis D, Kerveno M, Kossionides E, Kratička M, Lamboudis C, Leeb H, Lindote A, Lopes I, Lukic S, Marganiec J, Marrone S, Martínez T, Massimi C, Mastinu P, Mengoni A, Moreau C, Mosconi M, Neves F, Oberhummer H, O'Brien S, Pancin J, Papachristodoulou C, Papadopoulos C, Paradela C, Patronis N, Pavlik A, Pavlopoulos P, Perrot L, Pigni M T, Plag R, Plompen A, Plukis A, Poch A, Praena J, Pretel C, Quesada J, Reifarh R, Rosetti M, Rubbia C, Rudolf G, Rullhusen P, Salgado J, Santos C, Sarchiapone L, Savvidis I, Stephan C, Tain J L, Tassan-Got L, Tavora L, Terlizzi R, Vannini G, Vaz P, Ventura A, Villamarin D, Vincente M C, Vlachoudis V, Vlastou R, Voss F, Walter S, Wiescher M and Wisshak K 2011 *Phys. Rev. C* **84** 055802
- [205] Tagliente G, Milazzo P M, Fujii K, Abbondanno U, Aerts G, Álvarez H, Alvarez-Velarde F, Andriamonje S, Andrzejewski J, Audouin L, Badurek G, Baumann P, Bečvář F, Belloni F, Berthoumieux E, Calviño F, Calviani M, Cano-Ott D, Capote R, Carrapiço C, Cennini P, Chepel V, Chiaveri E, Colonna N, Cortes G, Couture A, Dahlfors M, David S, Dillmann I, Domingo-Pardo C, Dridi W, Duran I, Eleftheriadis C, Embid-Segura M, Ferrari A, Ferreira-Marques R, Furman W, Goncalves I, Gonzalez-Romero E, Gramegna F, Guerrero C, Günsing F, Haas B, Haight R, Heil M, Herrera-Martinez A, Jericha E, Käppeler F, Kadi Y, Karadimos D, Karamanis D, Kerveno M, Kossionides E, Kratička M, Lamboudis C, Leeb H, Lindote A, Lopes I, Lukic S, Marganiec J, Marrone S, Martínez T, Massimi C, Mastinu P, Mengoni A, Moreau C, Mosconi M, Neves F, Oberhummer H, O'Brien S, Papachristodoulou C, Papadopoulos C, Paradela C, Patronis N, Pavlik A, Pavlopoulos P, Perrot L, Pigni M T, Plag R, Plompen A, Plukis A, Poch A, Praena J, Pretel C, Quesada J, Reifarh R, Rosetti M, Rubbia C, Rudolf G,

- Rullhusen P, Salgado J, Santos C, Sarchiapone L, Savvidis I, Stephan C, Tain J L, Tassan-Got L, Tavora L, Terlizzi R, Vannini G, Vaz P, Ventura A, Villamarin D, Vincente M C, Vlachoudis V, Vlastou R, Voss F, Walter S, Wiescher M and Wisshak K 2013 *Phys. Rev. C* **87** 014622
- [206] Terlizzi R, Abbondanno U, Aerts G, Álvarez H, Alvarez-Velarde F, Andriamonje S, Andrzejewski J, Assimakopoulos P, Audouin L, Badurek G, Baumann P, Bečvář F, Berthoumieux E, Calviani M, Calviño F, Cano-Ott D, Capote R, Albornoz A C D, Cennini P, Chepel V, Chiaveri E, Colonna N, Cortes G, Couture A, Cox J, Dahlfors M, David S, Dillmann I, Dolfini R, Domingo-Pardo C, Dridi W, Duran I, Eleftheriadis C, Embid-Segura M, Ferrant L, Ferrari A, Ferreira-Marques R, Fitzpatrick L, Frais-Koelbl H, Fujii K, Furman W, Gallino R, Goncalves I, Gonzalez-Romero E, Goverdovski A, Gramegna F, Griesmayer E, Guerrero C, Gunsing F, Haas B, Haight R, Heil M, Herrera-Martinez A, Igashira M, Isaev S, Jericha E, Kadi Y, Käppeler F, Karamanis D, Karadimos D, Kerveno M, Ketlerov V, Koehler P, Konovalov V, Kossionides E, Krtička M, Lamboudis C, Leeb H, Lindote A, Lopes I, Lozano M, Lukic S, Marganec J, Marques L, Marrone S, Massimi C, Mastinu P, Mengoni A, Milazzo P M, Moreau C, Mosconi M, Neves F, Oberhummer H, O'Brien S, Pancin J, Papachristodoulou C, Papadopoulos C, Paradela C, Patronis N, Pavlik A, Pavlopoulos P, Perrot L, Pignatari M, Plag R, Plompen A, Plukis A, Poch A, Pretel C, Quesada J, Rauscher T, Reifarh R, Rosetti M, Rubbia C, Rudolf G, Rullhusen P, Salgado J, Sarchiapone L, Savvidis I, Stephan C, Tagliente G, Tain J L, Tassan-Got L, Tavora L, Vannini G, Vaz P, Ventura A, Villamarin D, Vincente M C, Vlachoudis V, Vlastou R, Voss F, Walter S, Wendler H, Wiescher M and Wisshak K 2007 *Phys. Rev. C* **75** 035807
- [207] Lederer C, Colonna N, Domingo-Pardo C, Gunsing F, Käppeler F, Massimi C, Mengoni A, Wallner A and the n.TOF Collaboration 2011 *Phys. Rev. C* **83** 034608
- [208] Domingo-Pardo C, Abbondanno U, Aerts G, Álvarez H, Alvarez-Velarde F, Andriamonje S, Andrzejewski J, Assimakopoulos P, Audouin L, Badurek G, Baumann P, Bečvář F, Berthoumieux E, Bisterzo S, Calviño F, Calviani M, Cano-Ott D, Capote R, Carrapiço C, Cennini P, Chepel V, Chiaveri E, Colonna N, Cortes G, Couture A, Cox J, Dahlfors M, David S, Dillman I, Dolfini R, Dridi W, Duran I, Eleftheriadis C, Embid-Segura M, Ferrant L, Ferrari A, Ferreira-Marques R, Fitzpatrick L, Frais-Koelbl H, Fujii K, Furman W, Gallino R, Goncalves I, Gonzalez-Romero E, Goverdovski A, Gramegna F, Griesmayer E, Guerrero C, Gunsing F, Haas B, Haight R, Heil M, Herrera-Martinez A, Igashira M, Isaev M, Jericha E, Käppeler F, Kadi Y, Karadimos D, Karamanis D, Kerveno M, Ketlerov V, Koehler P, Konovalov V, Kossionides E, Krtička M, Lamboudis C, Leeb H, Lindote A, Lopes I, Lozano M, Lukic S, Marganec J, Marrone S, Massimi C, Mastinu P, Mengoni A, Milazzo P M, Moreau C, Mosconi M, Neves F, Oberhummer H, Oshima M, O'Brien S, Pancin J, Papachristodoulou C, Papadopoulos C, Paradela C, Patronis N, Pavlik A, Pavlopoulos P, Perrot L, Plag R, Plompen A, Plukis A, Poch A, Pretel C, Quesada J, Rauscher T, Reifarh R, Rosetti M, Rubbia C, Rudolf G, Rullhusen P, Salgado J, Sarchiapone L, Savvidis I, Stephan C, Tagliente G, Tain J L, Tassan-Got L, Tavora L, Terlizzi R, Vannini G, Vaz P, Ventura A, Villamarin D, Vincente M C, Vlachoudis V, Vlastou R, Voss F, Walter S, Wendler H, Wiescher M and Wisshak K 2007 *Phys. Rev. C* **76** 045805
- [209] Domingo-Pardo C, Abbondanno U, Aerts G, Álvarez-Pol H, Alvarez-Velarde F, Andriamonje S, Andrzejewski J, Assimakopoulos P, Audouin L, Badurek G, Baumann P, Bečvář F, Berthoumieux E, Calviño F, Cano-Ott D, Capote R, Albornoz A C D, Cennini P, Chepel V, Chiaveri E, Colonna N, Cortes G, Couture A, Cox J, Dahlfors M, David S, Dillman I, Dolfini R, Dridi W, Duran I, Eleftheriadis C, Embid-Segura M, Ferrant L, Ferrari A, Ferreira-Marques R, Fitzpatrick L, Frais-Koelbl H, Fujii K, Furman W, Gallino R, Goncalves I, Gonzalez-Romero E, Goverdovski A, Gramegna F, Griesmayer E, Guerrero C, Gunsing F, Haas B, Haight R, Heil M, Herrera-Martinez A, Igashira M, Isaev S, Jericha E, Kadi Y, Käppeler F, Karamanis D, Karadimos D, Kerveno M, Ketlerov V, Koehler P, Konovalov V, Kossionides E, Krtička M, Lamboudis C, Leeb H, Lindote A, Lopes I, Lozano M, Lukic S, Marganec J,

- Marques L, Marrone S, Mastinu P, Mengoni A, Milazzo P M, Moreau C, Mosconi M, Neves F, Oberhummer H, Oshima M, O'Brien S, Pancin J, Papachristodoulou C, Papadopoulos C, Paradela C, Patronis N, Pavlik A, Pavlopoulos P, Perrot L, Plag R, Plompen A, Plukis A, Poch A, Pretel C, Quesada J, Rauscher T, Reifarth R, Rosetti M, Rubbia C, Rudolf G, Rullhusen P, Salgado J, Sarchiapone L, Savvidis I, Stephan C, Tagliente G, Tain J L, Tassan-Got L, Tavora L, Terlizzi R, Vannini G, Vaz P, Ventura A, Villamarin D, Vincente M C, Vlachoudis V, Vlastou R, Voss F, Walter S, Wendler H, Wiescher M and Wisshak K 2006 *Phys. Rev. C* **74** 025807
- [210] Massimi C, Koehler P, Bisterzo S and the n_TOF collaboration 2012 *Phys. Rev. C* **85** 044615
- [211] Mosconi M, Fujii K, Mengoni A, Heil M, Käppeler F and n_TOF Collaboration) T 2010 *Phys. Rev. C* **82** 015802
- [212] Mosconi M, Heil M, Käppeler F and Mengoni A 2010 *Phys. Rev. C* **82** 015803
- [213] Fujii K, Mosconi M, Mengoni A and et a 2010 *Phys. Rev. C* **82** 015804
- [214] Lederer C, Massimi C, Altstadt S, Andrzejewski J, Audouin L, Barbagallo M, Bécares V, Bečvář F, Belloni F, Berthoumieux E, Billowes J, Boccone V, Bosnar D, Brugger M, Calviani M, Calviño F, Cano-Ott D, Carrapiço C, Cerutti F, Chiaveri E, Chin M, Colonna N, Cortés G, Cortés-Giraldo M A, Diakaki M, Domingo-Pardo C, Duran I, Dressler R, Dzysiuk N, Eleftheriadis C, Ferrari A, Fraval K, Ganesan S, García A R, Giubrone G, Gómez-Hornillos M B, Gonçalves I F, González-Romero E, Griesmayer E, Guerrero C, Günsing F, Gurusamy P, Jenkins D G, Jericha E, Kadi Y, Käppeler F, Karadimos D, Kivel N, Koehler P, Kokkoris M, Korschinek G, Krtička M, Kroll J, Langer C, Leeb H, Leong L S, Losito R, Manousos A, Marganec J, Martínez T, Mastinu P F, Mastromarco M, Meaze M, Mendoza E, Mengoni A, Milazzo P M, Mingrone F, Mirea M, Mondelaers W, Paradela C, Pavlik A, Perkowski J, Pignatari M, Plompen A, Praena J, Quesada J M, Rauscher T, Reifarth R, Riego A, Roman F, Rubbia C, Sarmiento R, Schillebeeckx P, Schmidt S, Schumann D, Tagliente G, Tain J L, Tarrío D, Tassan-Got L, Tsinganis A, Valenta S, Vannini G, Variale V, Vaz P, Ventura A, Versaci R, Vermeulen M J, Vlachoudis V, Vlastou R, Wallner A, Ware T, Weigand M, Weiß C, Wright T J and Žugec P 2013 *Phys. Rev. Lett.* **110** 022501
- [215] Abbondanno U, Aerts G, Alvarez H, Andriamonje S, Angelopoulos A, Assimakopoulos P, Bacri C O, Badurek G, Baumann P, Becvar F, Beer H, Benlliure J, Berthier B, Berthoumieux E, Bertuzzi J, Blanc D, Bonzano R, Borcea C, Bourquin P, Bustreo N, Buttkus J, Calvino F, Cano-Ott D, Capote R, Cappi R, Carlier J, Carlson P, Cennini E, Cennini P, Chapuis D, Chepel V, Chiaveri E, Chohan V, Coceva C, Colonna N, Come J, Cortes G, Cortina D, Couture A, Cox J, Dababneh S, Daems G, Dahlfors M, Dangendorf V, David S, Dobers C, Dolfini R, Domingo-Pardo C, Duran-Escribano I, Durieu L, Eleftheriadis C, Embid-Segura M, Ferrant L, Ferrari A, Ferreira-Lorenzo L, Ferreira-Marques R, Flamant C, Frais-Koelbl H, Furman W, Gaidon M, Gascon J, Gasser D, Giomataris Y, Giovannozzi M, Goncalves I, Gonzalez-Romero E, Goulas I, Goverdovski A, Gramegna F, Griesmayer E, Günsing F, Haight R, Heil M, Herrera-Martinez A, Ioannides K, Janeva N, Jericha E, Kadi Y, Käppeler F, Karamanis D, Kelic A, Ketlerov V, Kitis G, Koehler P, Konovalov V, Kossionides E, Kowalik G, Kuhl-Kinell J, Lacoste V, Lacroix J, Leeb H, Lindote A, Lopes I, Lozano M, Lukic S, Magnin R, Mahner E, Marie F, Markov S, Marrone S, Martinez-Val J, Mastinu P, Mengoni A, Messerli R, Metral G, Milazzo P, Minguez E, Molina-Coballes A, Monteiro J, Moreau C, Neves F, Niquevert B, Nolte R, Oberhummer H, O'Brien S, Pancin J, Paradela-Dobarro C, Pavlik A, Pavlopoulos P, Perez-Parra A, , Perlado J, Perrot L, Peskov V, Plag R, Plompen A, Plukis A, Poch A, Poehler M, Policarpo A, Pretel C, Quesada J, Radermacher E, Raich U, Raman S, Rapp W, Rauscher T, Reifarth R, Rejmund F, Riunaud J, Rollinger G, Rosetti M, Rubbia C, Rudolf G, Rullhusen P, Saldana F, Salgado J, Savvidis E, Silari M, Soares J, Stephan C, Tagliente G, Tain J, Tapia C, Tassan-Got L, Tavora L, Terlizzi R, Terrani M, Tsangas N, Van Baaren W, Vannini G, Vaz P, Ventura A, Villamarin-Fernandez D, Vicente-Vicente M, Vlachoudis V, Vlastou R, Voss F, Weierganz M, Wendler H, Wiescher M, Wisshak K, Zanini L and Zanolli M 2004 *Phys. Rev. Lett.* **93** 161103

- [216] Marrone S, Abbondanno U, Aerts G, Alvarez-Velarde F, Alvarez-Pol H, Andriamonje S, Andrzejewski J, Badurek G, Baumann P, Becvar F, Benlliure J, Berthomieux E, Calvino F, Cano-Ott D, Capote R, Cennini P, Chepel V, Chiaveri E, Colonna N, Cortes G, Cortina D, Couture A, Cox J, Dababneh S, Dahlfors M, David S, Dolfini R, Domingo-Pardo C, Duran-Escribano I, Embid-Segura M, Ferrant L, Ferrari A, Ferreira-Marques R, Fraix-Koelbl H, Fujii K, Furman W I, Gallino R, Goncalves I F, Gonzalez-Romero E, Goverdovski A, Gramegna F, Griesmayer E, Gunsing F, Haas B, Haight R, Heil M, Herrera-Martinez A, Isaev S, Jericha E, Kappeler F, Kadi Y, Karadimos D, Kerveno M, Ketlerov V, Koehler P E, Kononov V, Kritcka M, Lamboudis C, Leeb H, Lindote A, Lopes M I, Lozano M, Lukic S, Marganec J, Martinez-Val J, Mastinu P F, Mengoni A, Milazzo P M, Molina-Coballes A, Moreau C, Mosconi M, Neves F, Oberhummer H, O'Brien S, Pancin J, Papaevangelou T, Paradela C, Pavlik A, Pavlopoulos P, Perlado J M, Perrot L, Pignatari M, Pigni M T, Plag R, Plompen A, Plukis A, Poch A, Policarpo A, Pretel C, Quesada J M, Raman S, Rapp W, Rauscher T, Reifarh R, Rosetti M, Rubbia C, Rudolf G, Rullhusen P, Salgado J, Soares J C, Stephan C, Tagliente G, Tain J L, Tassan-Got L, Tavora L M N, Terlizzi R, Vannini G, Vaz P, Ventura A, Villamarin-Fernandez D, Vincente-Vincente M, Vlachoudis V, Voss F, Wandler H, Wiescher M, Wisshak K and n TOF Collaborat 2006 *Phys. Rev. C* **73** 034604
- [217] Koehler P, Graff S, O'Brian H, Gledenov Y and Popov Y 1993 *Phys. Rev. C* **47** 2107 – 2112
- [218] Koehler P, Kavanagh R, Vogelaar R, Gledenov Y and Popov Y 1997 *Phys. Rev. C* **56** 1138–1143
- [219] Weigand M, Bredeweg T, Couture A, Jandel M, Käppeler F, Lederer C, Korschinek G, Krticka M, O'Donnell J, Reifarh R, Ullmann J and Wallner A 2010 *Nuclei in the Cosmos-XII* <http://pos.sissa.it/> ed Lugaro M and Lattanzio J (SISSA, Trieste: Proceedings of Science) contr. 184
- [220] Koehler P E, Reifarh R, Ullmann J L, Bredeweg T A, O'Donnell J M, Rundberg R S, Vieira D J and Wouters J M 2012 *Physical Review Letters* **108**(14) 142502
- [221] Reifarh R, Agvaanlvsan U, Alpizar-Vicente A, Bredeweg T, Esch E I, Greife U, Haight R, Hatarik R, Herwig F, O'Donnell J, Rundberg R, Schwantes J, Ullmann J, Vieira D and Wouters J 2006 *New Astronomy Reviews* **50** 644647
- [222] Kimura A, Furutaka K, Goko S, Harada H, Kin T, Kitatani F, Koizumi M, Nakamura S, Ohta M, Toh Y, Fujii T, Fukutani S, Hori J, Takamiya K, Igashira M, Katabuchi T, Mizumoto M, Kamiyama T, Kino K and Kuynagi Y 2011 *Journal of the Korean Physical Society* **59** 1828
- [223] <http://www.phy.ornl.gov/orela/orela.html/>
- [224] Macklin R, Halperin J and Winters R 1979 *Nucl. Instr. Meth. A* **164** 213
- [225] Macklin R, Halperin J and Winters R 1975 *Phys. Rev. C* **11** 1270
- [226] Macklin R, Halperin J and Winters R 1977 *Ap. J.* **217** 222
- [227] Macklin R and Young P 1987 *Nucl. Sci. Eng.* **97** 239 – 244
- [228] Macklin R 1988 *Nucl. Sci. Eng.* **99** 133
- [229] Macklin R 1982 *Nucl. Sci. Eng.* **81** 520
- [230] Macklin R 1983 *Nucl. Sci. Eng.* **85** 350
- [231] Macklin R 1985 *Nucl. Sci. Eng.* **89** 79
- [232] Macklin R 1985 *Astrophys. Space Sci.* **115** 71
- [233] Koehler P, Spencer R, Winters R, Guber K, Harvey J, Hill N and Smith M 1997 *Nucl. Phys.* **A621** 258c – 261c
- [234] Koehler P, Spencer R, Guber K, Winters R, Raman S, Harvey J, Hill N, Blackmon J, Bardayan D, Larson D, Lewis T, Pierce D and Smith M 1998 *Phys. Rev. C* **57** R1558 – R1561
- [235] Koehler P, Winters R, Guber K, Rauscher T, Harvey J, Raman S, Spencer R, Blackmon J, Larson D, Bardayan D and Lewis T 2001 *Phys. Rev. C* **63** 049901
- [236] Rapp W, Koehler P, Käppeler F and Raman S 2003 *Phys. Rev. C* **68** 015802
- [237] Koehler P E, Gledenov Y M, Rauscher T and Fröhlich C 2004 *Phys. Rev. C* **69** 15803
- [238] Koehler P E and Guber K H 2013 *Phys. Rev. C* **88** 035802
- [239] Bensussan A and Salome J 1978 *Nucl. Instr. Meth.* **155** 11

- [240] Block R, Danon Y, Gunsing F and Haight R 2009 *Handbook of Nuclear Engineering, Vol. I* (Berlin: Springer) ISBN: 9780387981307
- [241] Guber K, Koehler P, Derrien H, Valentine T, Leal L and Sayer R 2003 *Phys. Rev. C* **67** 062802
- [242] Mutti P, Beer H, Brusegan A, Corvi F and Gallino R 2005 *Nuclear Data for Science and Technology* AIP Conference Series 769 ed Haight R, Chadwick M, Kawano T and Talou P (New York: AIP) pp 1327 – 1330
- [243] Guber K, Spencer R, Koehler P and Winters R 1997 *Phys. Rev. Lett.* **78** 2704 – 2707
- [244] Beer H, Corvi F and Mutti P 1997 *Ap. J.* **474** 843 – 861
- [245] Wagemans C, Wagemans J, Goeminne G, Serot O, Loiselet M and Gaelens M 202 *Phys. Rev. C* **65** 034614
- [246] De Smet L, Wagemans C, Goeminne G, Heyse J and Van Gils J 2007 *Phys. Rev. C* **75** 034617
- [247] Beyer R, Birgersson E, Elekesa Z, Ferrari A, Grosse E, Hannaske R, Junghans A, Kögler T, Massarczyk R, Matica A, Nolte R, Schwengner R and Wagner A 2013 *Nucl. Instr. Meth. A* **723** 151
- [248] Bergman A and et al 1955 *Peaceful Uses of Atomic Energy, Vol. 4* (Geneva: United Nations) p 135
- [249] Abánades A, Aleixandre J, Andriamonje S and the TARC Collaboration 2002 *Nucl. Instrum. Methods Phys. Res. A* **478** 577–730
- [250] Rochman D, Haight R, O'Donnell J, Michaudon A, Wender S, Vieira D, Bond E, Bredeweg T, Kronenberg A, Wilhelmy J, Ethvignot T, Granier T, Petit M and Danon Y 2005 *Nucl. Instr. Meth. A* **550** 397 ISSN 0168-9002 URL <http://www.sciencedirect.com/science/article/pii/S0168900205012283>
- [251] Yamanaka A, Kimura I, Kanazawa S, Kobayashi K, Yamamoto S, Nakagome Y, Fujita Y and Tamai T 1993 *Journal of Nuclear Science and Technology* **30** 863–869 (Preprint <http://www.tandfonline.com/doi/pdf/10.1080/18811248.1993.9734560>) URL <http://www.tandfonline.com/doi/abs/10.1080/18811248.1993.9734560>
- [252] Maguire H, Stopa C, Block R, Harris D, Slovacek R, Dabbs J, Dougan R, Hoff R and Lougheed R 1985 *Nucl. Sci. Eng.* **89** 293–304 ISSN 0029-5639
- [253] Kobayashi K, Lee S, Yamamoto S, Cho H and Fujita Y 2002 *Journal of Nuclear Science and Technology* **39** 111–119 (Preprint <http://www.tandfonline.com/doi/pdf/10.1080/18811248.2002.9715164>) URL <http://www.tandfonline.com/doi/abs/10.1080/18811248.2002.9715164>
- [254] Reifarh R, Haight R, Heil M, Käppeler F and Vieira D 2003 *Nucl. Instr. Meth. A* **524** 215 – 226
- [255] Wisshak K, Voss F, Theis C, Käppeler F, Guber K, Kazakov L, Kornilov N and Reffo G 1996 *Phys. Rev. C* **54** 1451 – 1462
- [256] Wisshak K, Voss F, Käppeler F and Reffo G 1992 *Phys. Rev. C* **45** 2470 – 2486
- [257] Reifarh R, Käppeler F, Voss F, Wisshak K, Gallino R, Pignatari M and Straniero O 2004 *Ap. J.* **614** 363 – 370
- [258] Voss F, Wisshak K, Guber K, Käppeler F and Reffo G 1994 *Phys. Rev. C* **50** 2582 – 2601
- [259] Wisshak K, Guber K, Voss F, Käppeler F and Reffo G 1993 *Phys. Rev. C* **48** 1401 – 1419
- [260] Wisshak K, Voss F, Käppeler F, Guber K, Kazakov L, Kornilov N, Uhl M and Reffo G 1995 *Phys. Rev. C* **52** 2762–2779
- [261] Wisshak K, Voss F, Käppeler F and Kazakov L 2006 *Phys. Rev. C* **73** 015807
- [262] Wisshak K, Voss F, Käppeler F and Kazakov L 2002 *Phys. Rev. C* **66** 025801 (11)
- [263] Wisshak K, Voss F, Arlandini C, Bečvář F, Straniero O, Gallino R, Heil M, Käppeler F, Krτίčka M, Masera S, Reifarh R and Travaglio C 2001 *Phys. Rev. Lett.* **87** 251102 (4)
- [264] Wisshak K, Voss F, Arlandini C, Heil M, Käppeler F, Reifarh R, Bečvář F and Krτίčka M 2004 *Phys. Rev. C* **69** 055801 (12)
- [265] Reifarh R, Heil M, Käppeler F and Plag R 2009 *Nucl. Instr. Meth. A* **608** 139
- [266] Wisshak K and Käppeler F 1981 *Nucl. Sci. Eng.* **77** 58–70
- [267] Nagai Y, Igashira M, Mukai N, Ohsaki T, Uesawa F, Takeda K, Ando T, Kitazawa H, Kubono

- S and Fukuda T 1991 *Ap. J.* **381** 444–448
- [268] Ohsaki T, Nagai Y, Igashira M, Shima T, Seino S and Irie T 1994 *Ap. J.* **422** 912
- [269] Shima T, Okazaki F, Kikuchi T, Kobayashi T, Kii T, Baba T, Y N and Igashira M 1997 *Nucl. Phys.* **A621** 231c
- [270] Igashira M, Nagai Y, Masuda K, Ohsaki T and Kitazawa H 1995 *Ap. J.* **441** L89 – L92
- [271] Bradley T, Parsa Z, Stelts M and Chrien R 1979 *Nuclear Cross Sections for Technology (NBS Special Publication vol 594)* ed Fowler J L, Johnson C H and Bowman C D (Washington D.C.: National Bureau of Standards) p 344
- [272] Gritzay O, Koloty V, Klimova N, Kalchenko O, Gnidak M and Corona P 2008 *Nuclear Data for Science and Technology* ed Bersillon O, Gunsing F, Bauge E, Jaqmin R and Leray S (Paris: EDP Sciences) p 543
- [273] Gritzay O 2011 *Neutron Sources Spectra for EXFOR* INDC(NDS)-0590 ed Simakov S and Käppeler F (Vienna: IAEA) p 21
- [274] Couture A and Reifarh R 2007 *Atomic Data Nucl. Data Tables* **93** 807–830
- [275] Rauscher T and Thielemann F K 2000 *Atomic Data Nucl. Data Tables* **75** 1
- [276] Rauscher T 2012 *Ap. J. Lett.* **755** L10
- [277] Rauscher T 2012 code smaragd, version 0.9.0s unpublished
- [278] Goriely S 2005 Most statistical model code, version 2005 Tech. rep. <http://www-astro.ulb.ac.be>
- [279] Koning A, Hilaire S and Duijvestijn M 2005 *International Conference on Nuclear Data for Science and Technology* ed Haight R, Chadwick M, Kawano T and Talou P (New York: American Institute of Physics) pp 1154–1157 AIP Conference Series 769
- [280] Frenje J A, Bionta R, Bond E J, Caggiano J A, Casey D T, Cerjan C, Edwards J, Eckart M, Fittinghoff D N, Friedrich S, Glebov V Y, Glenzer S, Grim G, Haan S, Hatarik R, Hatchett S, Gatu Johnson M, Jones O S, Kilkenny J D, Knauer J P, Landen O, Leeper R, Le Pape S, Lerche R, Li C K, Mackinnon A, McNaney J, Merrill F E, Moran M, Munro D H, Murphy T J, Petrasso R D, Rygg R, Sangster T C, Séguin F H, Sepke S, Spears B, Springer P, Stoeckl C and Wilson D C 2013 *Nuclear Fusion* **53** 043014
- [281] Takahashi K and Yokoi K 1987 *Atomic Data Nucl. Data Tables* **36** 375
- [282] Goriely S 1999 *Astron. Astrophys.* **342** 881
- [283] Klay N and Käppeler F 1988 *Phys. Rev. C* **38** 295 – 306
- [284] Jung M, Bosch F, Beckert K, Eickhoff H, Folger H, Franzke B, Gruber A, Kienle P, Klepper O, Koenig W, Kozhuharov C, Mann R, Moshhammer R, Nolden F, Schaaf U, Soff G, Spädke P, Steck M, Stöhlker T and Sümmerer K 1992 *Phys. Rev. Lett.* **69** 2164 – 2167
- [285] Bosch F, Faestermann T, Friese J, Heine F, Kienle P, Wefers E, Zeitelhack K, Beckert K, Franzke B, Klepper O, Kozhuharov C, Menzel G, Moshhammer R, Nolden F, Reich H, Schlitt B, Steck M, Stöhlker T, Winkler T and Takahashi K 1996 *Phys. Rev. Lett.* **77** 5190 – 5193
- [286] Faber M, Ivanov A, Kienle P, Kryshen E, Pitschmann M and Troitskaya N 2008 *Phys. Rev. C* **78** 061603(R)
- [287] Fuller G M, Fowler W A and Newman M J 1980 *Ap. J. Suppl.* **42** 447–473
- [288] Langanke K and Martínez-Pinedo G 2000 *Nuclear Physics A* **673** 481–508 (Preprint [arXiv: nuc1-th/0001018](https://arxiv.org/abs/nuc1-th/0001018))
- [289] Langanke K and Martínez-Pinedo G 2003 *Reviews of Modern Physics* **75** 819–862 (Preprint [arXiv: nuc1-th/0203071](https://arxiv.org/abs/nuc1-th/0203071))
- [290] Taddeucci T, Goulding C, Carey T, Byrd R, Goodman C, Gaarde C, Larsen J, Horen D, Rapaport J and Sugarbaker E 1987 *Nucl. Phys.* **A469** 125 – 172
- [291] Frekers D 2005 *Nucl. Phys. A* **752** 580c
- [292] Chiaveri E and for the n_TOF collaboration 2013 *Nuclear Data for Science and Technology 2013*
- [293] Reifarh R, Chau L P, Heil M, Käppeler F, Meusel O, Plag R, Ratzinger U, Schempp A and Volk K 2009 *PASA* **26** 255
- [294] Ratzinger U, Chau L, Meusel O, Schempp A, Volk K, Heil M, Käppeler F and Stieglitz R 2007 *Proceedings of the 18th International Collaboration on Advanced Neutron Sources, ICANS*

- XVIII <http://www.ihep.ac.cn/english/conference/icans/proceedings/indexed/copyr/31.pdf> ed Wei J, Wang S, Huang W and Zhao J (Beijing, China: Institute of High Energy Physics, Chinese Academy of Science) p 210
- [295] Chau L, Meusel O, Ratzinger U, Schempp A, Volk K and Heil M 2006 *EPAC Edinburgh 2006* p 1690 available online at <http://accelconf.web.cern.ch/AccelConf/e06/PAPERS/TUPLS082.PDF>
- [296] Meusel O, Chau L, Mueller I, Ratzinger U, Schempp A, Volk K, Zhang C and Minaev S 2006 *Linac 2006, Knoxville, USA* (<http://accelconf.web.cern.ch/AccelConf/106/PAPERS/MO051.PDF>) p 159
- [297] Wei J, Arenius D, Bernard E, Bultman N, Casagrande F, Chouhan S, Compton C, Davidson K, Facco A, Ganni V, Gibson P, Glasmacher T, Harle L, Holland K, Johnson M, Jones S, Leitner D, Leitner M, Machicoane G, Marti F, Morris D, Nolen J, Ozelis J, Peng S, Popielarski J, Popielarski L, Pozdeyev E, Russo T, Saito K, Webber R, Weisend J, Williams M, Yamazaki Y, Zeller A, Zhang Y and Zhao Q 2012 *Proceedings of HIAT 2012, Chicago, IL USA* vol MOB01 (North-Holland, Amsterdam: CERN) p <http://accelconf.web.cern.ch/accelconf/HIAT2012/papers/mob01.pdf>
- [298] Tanihata I 1998 *Journal of Physics G Nuclear Physics* **24** 1311–1323
- [299] Gutbrod H H 2006 Facility for antiproton and ion research fair baseline technical report, isbn-3-9811298-0-6 Tech. rep. <http://www.fair-center.eu/for-users/publications/fair-publications.html>
- [300] Nagler A, Mardor I, Berkovits D, Dunkel K, Pekeler M, Piel C, vom Stein P and Vogel H 2006 *2006 Linear Accelerator Conference* ed Busso M, Gallino R and Raiteri C (CERN: Joint Accelerator Conferences Website, JACoW) p 168 <http://accelconf.web.cern.ch/accelconf/106/PAPERS/MOP054.PDF>
- [301] Feinberg G, Paul M, Arenshtam A, Berkovits D, Kijel D, Nagler I and Silverman I 2009 *Nucl. Phys. A* **827** 590c
- [302] Mastinu P, Martín Hernández G and Praena J 2009 *Nucl. Instr. Meth. A* **601** 333–338
- [303] Mastinu P, Praena J, Martín Hernández G, Dzysiuk N, Prete G, Capote R, Pignatari M and Ventura A 2012 *Physics Procedia* **26** 261
- [304] Culbertson C, Green S, Mason A, Picton D, Baugh G, Hugtenburg R, Yina Z, Scott M and Nelson J 2004 *Applied Radiation and Isotopes* **61** 733–738
- [305] Domingo-Pardo C and Guerrero C Tan J December 2013 *n_TOF Collaboration Meeting* (Bologna)
- [306] Nakamura S, Furutaka K, Goko S, Harada H, Kimura A, Kin T, Kitatani F, Koizumi M, Ohta M, Oshima M, Toh Y, Hori J, Fujii T, Fukutani S, Takamiya K, Igashira M, Katabuchi T, Mizumoto M, Kamiyama T, Kino K and Kiyonagi Y 2011 *Journal of the Korean Physical Society* **59** 1773 – 1776
- [307] Woods P, Lederer C and Käppeler F 2012 Destruction of the cosmic gamma-ray emitter ^{26}Al by neutron-induced reactions Tech. rep. URL <http://cds.cern.ch/record/1410662?ln=en>
- [308] Schatz H, Käppeler F, Koehler P, Wiescher M and Trautvetter H P 1993 *Ap. J.* **413** 750 – 755
- [309] Paradela C, Tassan-Got L, Audouin L, Berthier B, Duran I, Ferrant L, Isaev S, Le Naour C, Stephan C, Tarrío D, Trubert D and the n_TOF collaboration 2010 *Phys. Rev. C* **82** 034601
- [310] Reifarh R, Schwarz K and Käppeler F 2000 *Ap. J.* **528** 573 – 581
- [311] Reifarh R and Litvinov Y A 2014 *Phys. Rev. ST Accel. Beams* **17**(1) 014701 URL <http://link.aps.org/doi/10.1103/PhysRevSTAB.17.014701>
- [312] Hillenbrand P M, Hagmann S, Stöhlker T, Litvinov Y, Kozhuharov C, Spillmann U, Shabaev V, Stiebing K, Lestinsky M, Surzhykov A, Voitkiv A, Franzke B, Fischer D, Brandau C, Schippers S, Mueller A, Schneider D, Jakubassa D, Artiomov A, DeFilippo E, Ma X, Dörner R and Rothard H 2013 *Physica Scripta Volume T* **156** 014087
- [313] von Hahn R, Berg F, Blaum K, Crespo Lopez-Urrutia J R, Fellenberger F, Froese M, Grieser M, Krantz C, Kühnel K U, Lange M, Menk S, Laux F, Orlov D A, Repnow R, Schröter C D, Shornikov A, Sieber T, Ullrich J, Wolf A, Rappaport M and Zajfman D 2011 *Nuclear Instruments and Methods in Physics Research B* **269** 2871–2874

- [314] Bao Z and Käppeler F 1987 *Atomic Data Nucl. Data Tables* **36** 411–451
- [315] Gallino R, Busso M, Picchio G, Raiteri C and Renzini A 1988 *Ap. J.* **334** L45
- [316] Hollowell D and Iben I 1988 *Ap. J.* **333** L25
- [317] Beer H, Voß F and Winters R 1992 *Ap. J. Suppl.* **80** 403
- [318] Dillmann I, Heil M, Käppeler F, Plag R, Rauscher T and Thielemann F K 2005 *Capture Gamma-Ray Spectroscopy and Related Topics* AIP Conference Series 819 ed Woehr A and Aprahamian A (New York: AIP) p 123 <http://www.kadonis.org>
- [319] Cristallo S, Gallino R, Straniero O, Piersanti L and Domínguez I 2006 *Mem. Soc. Astron. Italiana* **77** 774